3(2) PERIODICAL Hyogo Univ. of Agr. Science Repts.
3(2)
P. O. F. I. LIBRARY
OCT 13 1959
FISH & WILDLIFE SERVICE

兵庫農科大学研究報告

第3巻 第2号

ND
E
B

自然科学編

THE SCIENCE REPORTS OF THE HYOGO UNIVERSITY OF AGRICULTURE

Vol. 3 No. 2

Series: Natural Science

兵庫農科大学

昭和33年

Sasayama, Hyogo, Japan

1958

目　　次

藤田悦久：クロボシサルハムシの生活史 …… 17

樋口元亮・大平恭造・松居　弘・高沢一徳：Double Thin Lens 型 ß-Ray Spectrometer に於ける φ-Selection I（英文）…… 23

石田　裕：西日本産ナガゴミムシ属の新種について（英文）…… 32

石田　裕：日本産ガガンボ科目録及び属，亜属の検索 IV（英文）…… 37

CONTENTS

FUJITA, E: Life History of *Cryptosephalus signaticeps* BALY. (Coleoptera, Chrysomelidae). 17

HIGUCHI, M., OHIRA, K., MATSUI, H. and TAKAZAWA, K.: φ-Selection in a Double Thin Lens Beta-Ray Spectrometer. I. S-Focus. 23

ISHIDA, H. : Some New Species of the Genus *Pterostichus* from Western Japan. (Coleoptera : Harpalidae) 32

ISHIDA, H. : The Catalogue of the Japanese Tipulidae, With the Keys to the Genera and Subgenera (Diptera).
IV. Limoniinae, Tribe Pediciini. 37

クロボシサルハムシの生活史

藤　田　悦　久

Life history of *Cryptosephalus signaticeps* BALY

(Coleoptera, Chrysomelidae)

Etsuhisa FUJITA

卵，幼虫，蛹の時代を糞でつくられたケース（母虫は卵を自分の糞で完全につつみ，孵化幼虫はこれをさらに自分の排泄物で拡大しながら成長する）中で過す一群のハムシ（ツツハムシ群 *Camptostomes*）中，わが国で生活史が判明しているのはムシクソハムシ *Arthocephalus spliota*（BALY）（熊沢，1939）とバラルリサルハムシ *Cryptocephalus approximatus* BALY（永富，1953）のみである．

筆者はこれらハムシ類について細胞学的研究を行いつつある．そのため生活史の記されていないクロボシサルハムシ *Cryptocephalus signaticeps* BALY の飼育を行ったので，その概要を報告する．飼育は1957年5月から58年6月にかけて，兵庫県篠山町で行われたものである．

本文に入るに先だち，飼育の方法について教示を受け，かつ本稿の御校閲を頂いた本学昆虫学研究室永富昭氏，食草について教示を賜つた本学農場研究室小早川利次氏に対して謹んで感謝の意を表する．

成　虫

1）出現期　1958年の篠山における野外観察では4月中旬より6月下旬までみられ，5月上，中旬が最も多かつた．1957年に飼育を開始したもののうち♀6，♂7が58年4月14日から5月2日の間に羽化している．1958年4月24日から6月12日まで採集した成虫は♀33，♂31で，性比は1：1と考えられる．

2）寿命　1958年室内で羽化させた♀♂各6個体をコナラ *Quercus serrate* THUNB. の若い茎葉を入れたガラス円筒（18×25cm）中で飼育した結果は第1表の如く，♀♂共に平均40日位生存しているが，♀が多少長いようである．

3）産卵　羽化出現後，2～3日に交尾する．交尾様式は他のハムシ科甲虫の場合と同様である．交尾は日中時を選ばず，又期間中幾回となく行われる．1回の交尾時間は明確に観察できなかつたが，12時に交尾していたものが19時になつてもなお離れていなかつたので，バラルリハムシやムシクソハムシ同様相当長時間にわたるものと思われる．

Table 1. Longevity of adults

Sex	Date of Emergence		Longevity (days)
Female	April	20	16
	〃	20	49
	〃	23	50
	〃	23	43
	〃	24	48
	〃	29	34
		Mean	40
Male	April	14	21
	〃	16	43
	〃	20	43
	〃	22	47
	〃	29	38
	May	5	44
		Mean	39.3

前年から飼育羽化させたものをコナラの若葉を与えて産卵させた結果は，第2表の通りで，出現後約10日目より産卵をはじめ，全保卵数は個体により相当の差があるが，そのうちの96%前後を排出するようである．産卵は昼夜を問わず，連続30～40日にわたり行われる．しかし産卵せずに死ぬ♀もある．

産卵方法はバラルリハムシ同様で，母虫は自己の糞で卵を包被して落下させる．もつとも糞でつつまず，裸のまま産卵するときもある．

4）食性　本種の加害植物は広く，野外においてクリ *Castanea crenata* SIEB. et ZUCC.，クヌギ *Quercus acutissima* CARRUTH.，コナラ *Quercus serrate* THUNB.（以上ブナ科 *Fagaceae*），エゴノキ *Styrax japonica* SIEB. et ZUCC.（エゴノキ科 *Styracaceae*），ハンノキ

Table 2. Oviposition period and the number of deposited eggs.

Date	Rearing examples					
	1	2	3	4	5	6
Ⅳ 20	E	E				
21	0	0				
22	0	0				
23	0	0	E	E		
24	0	0	0	0	E	
25	0	0	0	0	0	
26	0	0	0	0	0	
27	0	0	0	0	0	
28	0	0	0	0	0	
29	0	0	0	0	0	E
30	0	0	0	2	0	0
Ⅴ 1	0	0	0	3	0	0
2	0	0	0	4	0	0
3	0	1	0	6	0	0
4	0	3	2	2	1	0
5	0	3	2	3	2	0
6	D	4	4	2	2	0
7		2	5	4	5	0
8		6	6	5	8	0
9		8	1	3	6	0
10		4	1	4	5	0
11		2	15	8	10	0
12		2	10+(2)	12	7	2
13		1	4	8	7	1
14		9	6	5	7	3+(1)
15		7	3	6	8	0
16		5	3	5	6	2
17		4	7	4	8	0
18		3	4	10	7	1
19		12	5	6	9	2+(1)
20		1	6	0	8	3
21		4	9	1	9+(1)	2
22		5	7	14	3	1
23		1	8+(1)	15	4+(1)	4
24		2	5	3	5	1
25		3	7+(1)	8	4	1
26		2	7	5	5	1
27		0	6	7	3	0
28		0	2	4	0	0
29		0	0	6	0	0
30		9	8	5	4	0
31		5	2	8	2	1
Ⅵ 1		8	3	4	3	D
2		(1)	0	0	D	
3		0	0	0		
4		0	0	0		

5			0	D	1		
6			5+(2)		2		
7			0		4		
8			0		4		
9			2		8		
10			0		13		
11			0		0		
12			D		D		
Oviposition period (days)		—	39	29	42	29	20
Number of deposited eggs		—	126	152	214	150	27
No. of eggs in ovary	Mature	33	6	7	5	5	2
	Immature	4	0	0	0	0	0
Total number of eggs		37	132	159	219	155	29

E: date of emergence, D: date of death.
Parenthesized number means the eggs without acase.

Alnus japonica (Thunb.) Steud. (ハンノキ科 *Betulaceae*) ノイバラ *Rosa multiflora* Thunb. (バラ科 *Rosaceae*) を食するのを観察している.

コナラで成虫を飼育したが, 主として若葉を好食し, 芽, 新茎, 枝の皮部を食することもある. 葉における食痕は不規則な班紋状を呈する.

卵

1) 形態 黄色, 鶏卵形である (Fig. 1). 殻には8～10条の凹んだ縦列が螺施状に走つている (Fig. 2). 大きさは第3表の通りである.

2) 卵期間 シヤーレ(7.5×2.5 cm)に土壌を浅く敷き, 卵をその上に置いた. 産卵されてから幼虫が糞殻外

Table. 3. Measurements of 28 eggs and their cases (mm).

		Min.	Max.	Mean
Case	Length	1.16	1.97	1.70
	Width	0.81	1.25	1.03
Egg	Length	0.84	1.06	0.98
	Width	0.44	0.50	0.47

Table 4. Incubation period of eggs

Month	No. of examined eggs	Period (days)			Mean temperature		
		Min.	Max.	Aver.	Min.	Max.	Aver.
V middle	91	27	32	29.6	14.3	17.6	16.2
V late	163	21	26	23.5	15.2	20.1	17.5
VI early	78	16	18	16.4	16	22	18.6

1

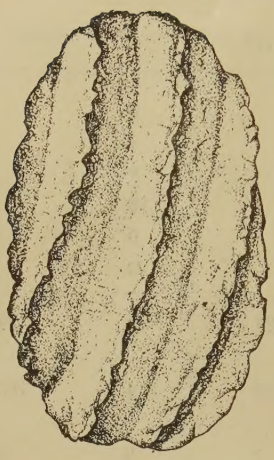

2

4

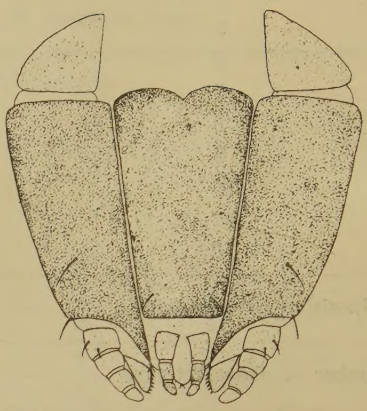

7

5

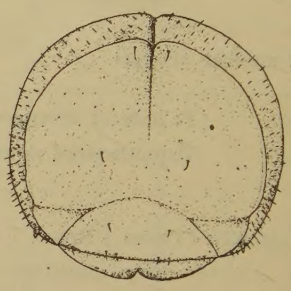

8

6

3

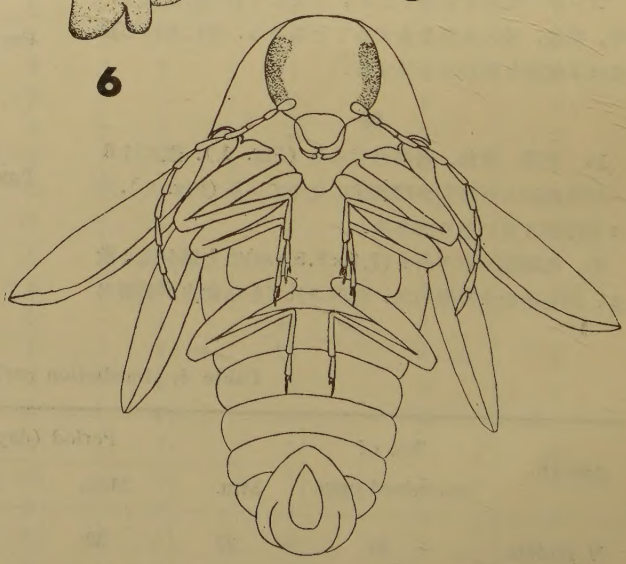

9

Explanation of Figures

1. The egg.
2. The case for egg.
3. The 5th inster larva.
4. The antenna of 5th inster larva.
5. The rigth mandible of 5th inster larva.
6. The left mandible of 5th inster larva.
7. The mouth part of 5th inster arva (Ventral aspect).
8. The head of 5th inster larva (Frontal aspect).
9. The pupa (Ventral aspect).

に頭を出すまでの期間を仮に卵期間とすると，1957年の調査結果は第4表の如く，気温の上昇により著しく短縮され，5月中旬と6月上旬では約2週間の差を生ずる．

幼　虫

1) 形態　5令幼虫の記載：体は略円筒形．頭は濃褐色，胸部及び腹部は帯黄白色で，胸部の硬皮板，胸脚，気門及び触角は薄褐色を呈する．

頭部は略円筒形で有毛，頬の部分に剛毛や微毛が最も多い．頭頂溝は深い．前額板は平滑であるが上方中央部に凹みがあり，2対の剛毛を有する．後頭板は中央部に1対，前縁に3対の剛毛を有し，前額板と頭楯板の分岐腺は不明瞭である．触角は無色で3節よりなり，第1節は太く長い．各節の長さの比は5：2：1である．上唇は細長く，上唇中央部は浅く凹み無毛である．額：頭楯：上唇＝18：8：3．大腮は黒褐色で太く短く，外側面に2～4の剛毛を有し，右は4歯，左は3歯を有する．小腮鬚基は濃褐色で大きく，2剛毛を生ずる．小腮鬚は薄褐色で4節からなり，第1節に2剛毛を有し，他は無毛である．外葉は褐色で三角状をなし，外側に6本の感覚毛を有し，内葉の先端周縁部に2剛毛を有する．下唇基は濃褐色で梯形に近く，上端中央部は凹みを生じ，前縁部に2対の剛毛を有する．下唇鬚は薄褐色で3節からなり無毛である．

胴部は3個の胸環及び8個の腹環節よりなり，腹部第5環節から腹方にJ字状に屈曲し，その屈曲点において最大に膨大している．全身に微毛又は剛毛を有し，前胸の硬皮板上及び尾節に最も密生している．第1胸環節背面に1対の硬皮板，第2，3胸環節には3対づつの硬皮板を有する．胸脚は4節で，跗節はするどくとがつた爪と融合し，第1節は第2，3，4各節に比して色が濃く，第1節には5剛毛，第2節には2剛毛，第3節には4剛毛，第4節には7剛毛を有する．各節の長さの比は前，中，後脚により外少異るが，大体13：4：10：9である．腹環節には1対の環状の気門があり，第1腹節～7腹節は5～7個の小環節からなつている．

体長は9.0～1.2mm（頭から第4腹節及び第5腹節から腹端まで夫々腹面に沿つて測定合計したもの）．殻長8.0～9.7mm，殻幅3.9～4.6mmに達する．

若令幼虫：1～4令は色，形共に5令とほとんど変りがない．

2) 殻の拡長　糞でつくられたケースの拡長機構はバラルリサルハムシ同様であるので，ここでは省略する．

3) 棲息場所及び食性　野外における幼虫の棲息場所及び食性は不明である．室内において，イタドリ *Polygonum cuspidatum* Sieb. et Zucc.（タデ科 *Polygonaceae*），クヌギ，クリの葉を与えて成長させた．生葉より枯葉をよく食し，枯枝の上皮も摂食する．イタドリの枯葉での飼育が最も良好であつた．葉脈は食さず網目状の食痕を残す．

幼虫は乾燥，多湿の環境下では成長不可能である．外国では本属（*Cryptocephalus*）の幼虫及び蛹が蟻の巣中で発見されている．しかし筆者の観察では，卵及び幼虫の附近にいる蟻はこれらに全く関心を示さなかつた．

4) 幼虫期間　1957年，室内飼育により幼虫の発育を観察した．脱皮回数は第5表の如く4回で5令を経過する．なお，表中に示した5令期間は第4回の脱皮から糞殻を閉鎖した時までを意味する．

孵化は5月中旬から6月下旬にわたつて行われるが，その後の発育には著しい個体変異がある．又幼虫の死亡率は非常に高く，飼育個体数約1000頭中，7月中旬（この頃3令）までに約⅘が死亡した．4，5令になると幾分多湿に耐えるようであるが，土壌，食草の乾燥に弱く，10月上旬最後の脱皮を行つて老熟し，幼虫態で越冬したものはわずか30数個体であつた．なお，3令で越冬した幼虫も12頭あつたが，これはその後全滅した（この中には翌年7月頃まで生存し殻の拡長を行つていたものもある）．2，3，4回目の脱皮をする時は自己の排泄物で糞殻の口を閉じ，脱皮後糞殻の口を開いて脱皮殻を外部に排出するが，第1回の脱皮の時は糞殻の口を閉ざさないようである．

Table. 5. Durations of larval stadia

Stage	Min.	Max.	Aver.	No. of examined specimens
1st	7	24	14.1	15
2nd	11	20	16.7	12
3rd	20	31	25.2	9
4th	30	58	33.6	8
5th	166	192	18.0	7

蛹

1957年，濾紙上で飼育した2頭の幼虫の記録によると，それぞれ羽化30，38日前に糞部を閉鎖し，体を反転して腹部を糞殻の開口部に向け蛹化する．糞殻閉鎖後蛹化するまでの日数は20，28日で真の蛹期間は12，10であつた．蛹の体は略長方形，体長5.5mm内外（アルコール

漬). 最初は体全体が淡黄白色であるが, 羽化前の着色は複眼に始まり, 大腮, 爪, 腿, 脛節基部, 触角, 前翅に及び漸次成体色に変色する.

羽化後, 3～4日糞殻中にいて, その一端を円形に切断して地表に現われる.

要　　約

1) 年1回の発生で, 成虫は篠山において5～6月にわたり出現する. 成虫期間は♀♂共に約40日, 卵期間は温度により異り16～30日, 幼虫期間は約9カ月, 前蛹期間は約25日, 蛹期間は約10日である.

2) 成虫は多食性で, ハンノキ, コナラ類等を食し, 卵を母虫の糞で包被して地上に落下させる.

3) 幼虫は5令を経過し, バラルリハムシ同様自分の排泄物で糞殻を拡張し, その糞殻中で生活する.

4) 幼虫は略円筒形, 腹部第5環節から腹方にJ字形に湾曲し, 各体節には微毛を有し, 特に頭部, 尾端に多い.

5) 野外における棲息場所及び食性は不明であるが, 室内では枯死したイタドリの葉における成長が最も良好であつた.　　(動物学講座, 1958年8月30日受理)

文　　献

1) 大井次三郎: 日本植物誌, 418, 423～424, 651, 934 (1953).

2) 中条道夫: 図説食葉はむし類, 65～72 (1956).

3) 熊沢隆義: 昆虫, **13** (1), 4～15 (1939).

4) 永富　昭: 昆虫, **20** (1.2), 6～8 (1953).

5) Peterson, A: *Larvae of Insects*, **11**, 148～149 (1953).

6) 湯浅啓温: 植物及動物, **2** (9), 111～112 (1934).

7) _____: 動物学雑誌, **55** (2), 46～47 (1943).

Résumé

The present paper deals with the life-history and early stages of *Cryptocephalus signaticeps* Baly observed at Sasayama, Hyogo prefecture, in 1957 and 1958.

The resalts are summrized as follows:

1). This beetle has one generation a year and the adult appears from April to June. The adult lives about 40 days in both sexes, the incubation period is 16 to 30 days according to tempreture, larval stage is about 9 months, prepupal stage is about 25 days and pupal stage is about 10 days.

2). The adult feeds on the leaves of chestnut' oak, alder etc.. The female encloses each egg with her excrement and drops it on the ground.

3). The larva has 5 instars. The larva gradually enlarges the case in the cousse of development, in such a way as observed already on the larva of *Cryptocephalus approximatus* Baly by Mr. Nagatomi (1953).

4). The larva is almost cylinder, J-shaped, curved ventrally at the fifth abdominal segment' scattered setae are present on most segment' especialy near the cepnalic and caudalends.

5). The habitat and feeding habit of the larva in the field are unknown. However, in laboratory the larva best feeds on the dead leaves of *Polygonum cuspidatum* Sieb. et Zucc. for sufficient nutrition. (Zoological laboratory)

φ—SELECTION IN A DOUBLE THIN LENS BETA-RAY SPECTROMETER I

S-FOCUS

M. Higuchi, K. Ohira, H. Matsui and K. Takazawa

Some difficulties that occur in the application of the φ-selection proposed by Jungerman and Beard to a double thin lens beta-ray spectrometer are described. One of the most important difficulties is that in a S-focus, in which the electrons emitted from the source points at various radius S of a large source are focused, available source radial width, ΔS, turns out to be smaller than the expected. Thus, in order to get the best focus mode based upon the φ-selection, the quantitative comparison between the S-focus including the first order α-focus and the complete α-focus including somewhat the S-focus should be made.

Introduction

One of the defects in helical spectrometers is that the point source must be used at high precision work. Though they have greater gathering power than that of flat spectrometers, luminosity turns out to be smaller on account of the small source area.

Hubert[1] has improved the line profile for a point source by originating the slit system that cut sharply higher momentum side. Adding, near the source, a cone shaped baffle[2] that cut the undesired ray (different momentum ray), we have successfully made the line profile for a finite source to be similar figures to that owing to Hubert slit system. Moreover, in order to increase the intensity, we have intended to use a ring source consisting of axial symmetric source points.

Recently Jungerman and Beard[3),4),5)] proposed an interesting idea about the improvement of the optimum condition in helical spectrometers. They introduced a new freedom φ, the angle made by the projection of the electron velocity vecter on a plane perpendicular to the instrument axis at the source with the radius of the source point, into the electron motion in the homogeneous magnetic field beta-ray spectrometers. It is shown that, by proper selection of the angle φ, an inverse 3/2 power dependence on the resolution is made possible by removing all dependence of the resolution on the source dimensions, thus enabling extremely large sources.

Both effects of a cone baffle and those of a ring source are comprehensible from this unified view point, φ-selection. Therefore we investigate theoretically and practically, how much inprovement is obtainable by the application of the S-focus, using the most promising fin baffle[5] for the φ-selection, to our double thin lens spectrometer.

Theoretical Consideration

It is assumed that the radial position of an electron, emitted from a source point located off the axis at radius S, is given approximately by

$$y \sim \rho + m\ (S,\ \alpha)\ S\cos\psi^* \qquad (1)$$

from the analogy to the case of homogeneous magnetic field spectrometers.[5] ρ is the radial position of the electron emitted from a point source and $\psi^* = \varphi + \psi$, ψ is the projected angular position (Fig. 1). m is the characteristic of non-homogeneous magnetic field spectrometers and is determined empirically from the calculated trajectories of $S=0.225$ cm, $\varphi=0$ ray and $S=0.350$ cm, $\varphi=0$ ray as follows

$$m = a\cos\alpha + bS + c \qquad (2)$$

α: emission angle
$a,\ b,\ c$: constants.

Though it is not a good approximation, Eq. (1) is adopted to carry out order estimation, since it is required to calculate numerically a number of angular momentum rays to proceed further approximation.

The change from a point source ray at the ring focus for a point source is given by

$$\Delta y = \frac{\partial y}{\partial k}\Delta k + \frac{\partial y}{\partial \alpha}\Delta\alpha + \frac{1}{2}\frac{\partial^2 y}{\partial \alpha^2}\Delta\alpha^2 + mS\cos\psi^*,$$

$$= \frac{\partial \rho}{\partial k}\Delta k - a\sin\alpha_0\ S\cos\psi^*\Delta\alpha + \frac{1}{2}\left(\frac{\partial^2\rho}{\partial\alpha^2} - a\cos\alpha_0\right.$$

$$\left. S\cos\psi^*\right)\Delta\alpha^2 + mS\cos\psi^*, \qquad (3)$$

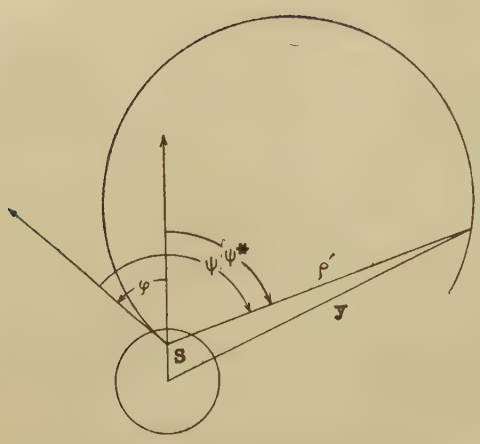

Fig. 1. Projection of electron trajectory on a plane perpendicular to the axis of the instrument.

where $k=p/i$, p is the electron momentum in $H\rho$ units and i is the magnetizing current in *amp*. The choice of $\varphi=\frac{\pi}{2}-\psi$ yields very small source effect, $mScos\psi^*$. Thus one obtains S-focus in addition to the first order focus of the emission angle.

The spread in $\Delta\alpha$ permitted by the Hubert slit system is given by

$$\Delta\alpha=\Delta\alpha_1+\Delta\alpha_2, \tag{4}$$

$$0=\frac{\partial\rho}{\partial k}\Delta k-asin\alpha_0Scos\psi^*\Delta\alpha_1+\frac{1}{2}\left(\frac{\partial^2\rho}{\partial\alpha^2}-acos\alpha_0Scos\psi^*\right)\Delta\alpha_1{}^2+mScos\psi^*, \tag{5}$$

$$0=\frac{\partial\rho}{\partial k}\Delta k+asin\alpha_0Scos\psi^*\Delta\alpha_2+\frac{1}{2}\left(\frac{\partial^2\rho}{\partial\alpha^2}-acos\alpha_0Scos\psi^*\right)\Delta\alpha_2{}^2+mScos\psi^*. \tag{6}$$

$\Delta\alpha_1$ and $\Delta\alpha_2$ are respectively the portion with larger emission angle and that with smaller emission angle than a standard one, 12°41′. Straightforward calculation shows that

$$\Delta\alpha=2\left(acos\alpha_0Scos\psi^*-\frac{\partial^2\rho}{\partial\alpha^2}\right)^{-1}\cdot\{2(\frac{\partial\rho}{\partial k}\Delta k+mScos\psi^*)\left(acos\alpha_0Scos\psi^*-\frac{\partial^2\rho}{\partial\alpha^2}\right)+(asin\alpha_0Scos\psi^*)^2\}^{\frac{1}{2}}. \tag{7}$$

Now let S_1 and S_2 be the inner and outer source radius and let X_m be the maximum value of $X=\left|\psi^*-\frac{\pi}{2}\right|$, the angular variation from the optimum value of $\psi^*=\frac{\pi}{2}$, permitted by the fin baffle. Therefore

$$\Delta\alpha=2\left(-\frac{\partial^2\rho}{\partial\alpha^2}\mp acos\alpha_0SX\right)^{-1}\{2(\frac{\partial\rho}{\partial k}\Delta k\mp mSX)\left(-\frac{\partial^2\rho}{\partial\alpha^2}\mp acos\alpha_0SX\right)+(asin\alpha_0SX)^2\}^{\frac{1}{2}}$$

$$(\psi^*=\frac{\pi}{2}\pm X). \tag{8}$$

According to the reference 5), the fraction of monoergic electrons emitted isotropically from the source which are counted is given as follows. For example, if $m(S_2)S_2X_m>\frac{\partial\rho}{\partial k}\Delta k>\frac{1}{2}\Delta y_p$:

$$I=\frac{1}{4\pi}\int_{S_{min}}^{S_{max}}2\pi SdS\int_0^{2\pi}\Delta\alpha sin\alpha_0d\psi^*$$

$$=\frac{sin\alpha_0}{2}\{\int_{S_1}^{A_1}SdS\int_{-X_m}^{X_m}\Delta\alpha(1-\frac{|X|}{X_m})dX+\int_{A_1}^{A_2}SdS\int_{-X_1}^{X_m}\Delta\alpha(1-\frac{|X|}{X_m})dX+\int_{A_2}^{S_2}SdS\int_{-X_1}^{X_2}\Delta\alpha(1-\frac{|X|}{X_m})dX\}, \tag{9}$$

$$A_1=\frac{1}{m(A_1)X_m}(\Delta y_p-\frac{\partial\rho}{\partial k}\Delta k)$$

Table I

S_2 (cm)	S_1 (cm)	X_m (rad.)	Δy_p (cm)	$m\frac{S_1+S_2}{2}X_m/\Delta y_p$	η (%)	I ($\times10^4$cm^2)	$\gamma\equiv I/\eta^{\frac{3}{2}}$ ($\times10$)
1.0	0	0.052	0.07	0.55	0.32	1.17	6.40
0.7	0	0.052	0.07	0.37	0.27	0.69	4.88
0.5	0	0.052	0.07	0.26	0.26	0.38	2.88
0.2	0	0.052	0.07	0.10	0.24	0.08	0.63
1.0	0	0.052	0.04	0.97	0.24	0.62	4.87
1.0	0.2	0.052	0.07	0.68	0.34	1.10	5.62
1.0	0.5	0.052	0.07	0.89	0.37	0.79	3.48
0.5	0.2	0.314	0.30	0.51	1.27	3.56	2.50

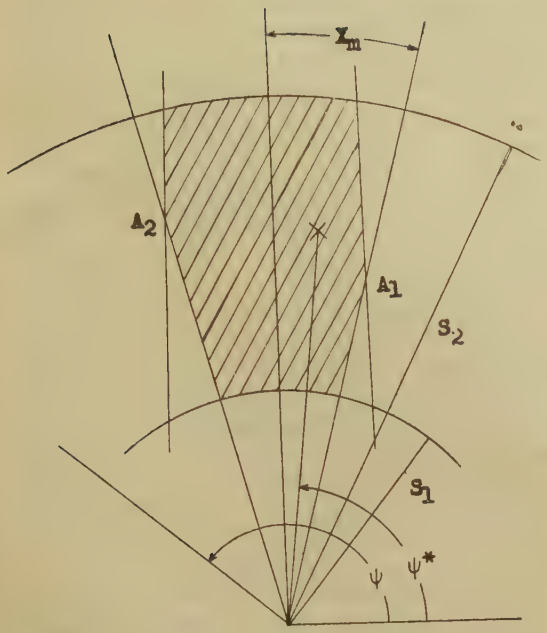

Fig. 2. Integration map (shaded area) for the source with φ-selecting fin baffle.

$$A_2=\frac{1}{m(A_2)X_m}\frac{\partial\rho}{\partial k}\Delta k$$

$$X_1=\frac{1}{m(S)S}(\Delta y_p-\frac{\partial\rho}{\partial k}\Delta k)$$

$$X_2=\frac{1}{m(S)S}\frac{\partial\rho}{\partial k}\Delta k.$$

The integration limits are shown in Fig. 2.

The results of the numerical surface integral are summarized in Table I and in Fig. 3. For example, a line profile for the case of $S_2=1.0$ cm, $S_1=0.5$ cm, $X_m=0.052$ radians and $\Delta y_p=0.07$ cm is shown in Fig. 4.

From these results the followings are observed;

1) The ratio γ of the peak intensity to the three-halves power of the relative half-maximum width η shows maximum at (*mean source effect*) $=0.55\sim0.6\times$ (*slit width*) for $S_1=0$ cm and $X_m=0.052$ radians. This fact should be compared with the case of the optimized Hubert system, (*source effect*) $=0.5\times$ (*slit width.*)
2) It seems likely that γ decreases with decreasing S_2/S_1.
3) The peak intensity is given by the formulae

$$I=\{1.10\frac{S_2}{\Delta y_p}-4.02\}\times10^{-5}\ cm^2$$

$$(S_2=0.5\rightarrow1.0,\ S_1=0)$$

$$I=\{6.42\left(\frac{S_2}{\Delta y_p}\right)^2+7.91\left(\frac{S_2}{\Delta y_p}\right)\}\times10^{-7}\ cm^2$$

$$(S_2=0.\rightarrow0.5,\ S_1=0). \qquad (10)$$

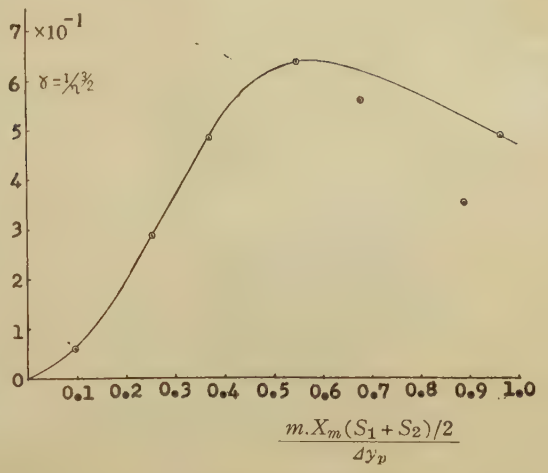

Fig. 3. γ *vs* mean source effect curve. γ shows maximum at 0.55~0.6. ($X_m=0.052$ radians)

4) The relative half-maximum width η is given by the formula

$$\eta=0.00038\left(\frac{S_2}{\Delta y_p}\right)^2+0.00042\left(\frac{S_2}{\Delta y_p}\right)+0.239\ \%$$

$$(S_1=0,\ X_m=0.052). \qquad (11)$$

From the comparison between the change of the radial position corresponding to the variation of ψ^*, $\Delta\psi^*=0.052$ radians, estimated from $mS\cos\psi^*$-approximation and the same one calculated by Keller's numerical method,[6] it becomes clear that the former is about two times larger than the latter. This means that the slit width on the integration map is underestimated by the factor~1/2. As the results of the correction for this error with the help of Eq. (10) and (11), the intensity I and the relative half-maximum width η, shown in Table I, must be multiplied respectively by ~4/3 and ~3/4. Choosing $S_2=1.0$ cm, $S_1=0$ cm, $X_m=0.052$ radians and $\Delta y_p=0.07$ cm, the improvement over the optimized Hubert system that is roughly estimated becomes ~12. As the realizable cases, for the case of $S_2=1.0$ cm, $S_1=0.5$ cm, $X_m=0.052$ radians and $\Delta y_p=0.07$ cm, the improvement over the 0.1 cm ϕ disc source with Hubert system is ~4. Thus it is expected theoretically that the considerable improvement is made possible by the application of the S-focus with the use of the φ-selecting fin baffle to our double thin lens beta-ray spectorometer.

Baffle Design

It is assumed that the electron of certain momentum k_0, emitted from any point on the source with the emission angle α_0, moves near the source on the surface of the cone of angle $2\alpha_0$, whose axis is

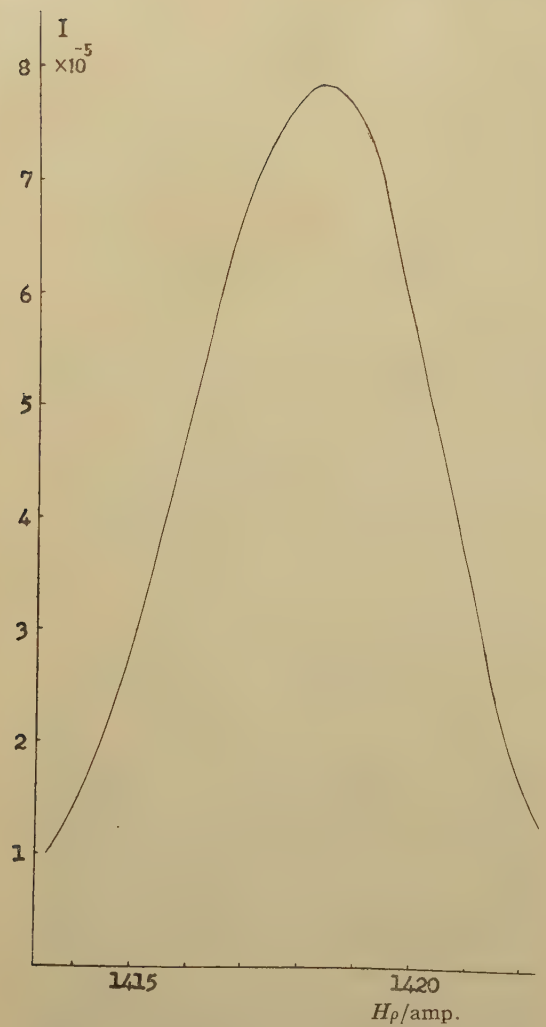

Fig. 4. Line profile for the case of $S_2=1.0$ cm, $S_1=0.5$ cm, $X_m=0.052$ radians and $\Delta y_p=0.07$ cm.

parallel to the field axis. And the rotating angle is assumed to be the same as that of the point source, ψ_0. For the present, an attempt of designing the φ-selecting baffle will be made on these assumptions.

Fig. 5 shows the electron position projected on the source plane perpendicular to the field axis. The points A_1 and C_1 represent the projected positions of the electrons at the axial distance z_0, originating from the source point A of radius S_0 with the emission angle α_0, in the directions of projected angles of φ_0 and φ_0+X_m, respectively. The value of φ_0 is chosen so as to make $cos\,(\varphi_0+\psi_{r0})$ vanish. The lines A_1A_2 and C_1C_2 parallel to OA represent the edges of the curved surfaces σ_1 and σ_2 involving the rays of φ_0 and φ_0+X_m, originating from the source line OA.

If the curved surfaces σ_1 and σ_2 from z_0 to source were used, the available source area should become to be infinitesimal small. Therefore, it is necessary to find the other baffle surface permitting the rays from some finite source area. For this purpose, we used the surface σ_1 and another curved surface σ_3, involvig the ray originating from a certain point C with φ_0 and having the edge parallel to OA at any axial distance. The point C is chosen so that the projected position of the electron at z_0 originating from this point C with φ_0 may be C_1.

When this curved surface σ_3 and the above mentioned σ_1 are used for baffles, these baffles permit the φ_0-rays with emission angle α_0, originating from any point on the source area OAB. And X_m is defined by the edges of these baffles at z_0. If we adopt the smaller value of z_0 ($\leq$2 cm), it is difficult to work the baffle because the slit width becomes so small, and if the larger value (>12cm), the above assumptions for the trajectory on the cone surface seem to be invalid.

When $z_0=12.1$ cm, $\alpha_0=12°41'$ and $S_0=1$ cm, the angle θ is obtained as 2°5′35″. The section of our baffle perpendicular to the instrumental axis has 86 slots, as shown in Fig. 6. In this case, a half of the source area is not available owing to the finite width of baffle walls. If the small source radius is utilized, the work of the baffle becomes difficult, so that the minimum source radius S_{min} is chosen as 0.5 cm. The outer radius r_{out} and inner radius r_{inn} of φ-selecting slits, indicated in Fig. 6, are determined so as to permit the α_{max} ($=14°35'$) and α_{min} ($=10°47'$) ray respectively.

In our actual design, piling 34 aluminum plates of 3 mm thickness with such 86 slots worked by cutter, a φ-baffle block is constructed.

Experiment

Fig. 7 shows the baffle geometry of our spectorometer near the ring slit for the point source, and the baffle R travels along the field axis to the position of R-1, R-2,···, etc.. Using a Cs^{137} ring source, of which inner radius 0.5 cm and outer radius 1 cm, the line profile of the 661 kev. K-internal coversion is obtained at the R-1 slit position, as represented by curve (1) of Fig. 8. This line profile have two large maxima owing to the use of the large ring source.

When the φ-baffle of 34 plates was set at the regular position in front of this ring source, the intensity of the experimental line profile was much weaker than expected. As shown by the curve (2) of Fig. 8, the maximum peak is found at 2.335 amp. and the resolution 0.5%. Removing ten and twenty source side plates from the φ-baffle block, the intensity of the line profile becomes larger step by step but these peak currents are almost the

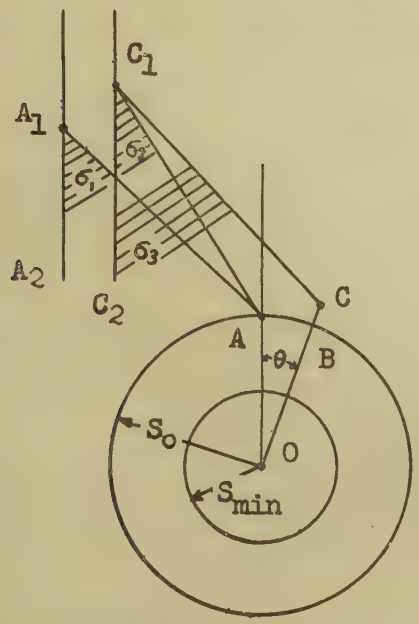

Fig. 5. Projection of curved surfaces used as baffle surfaces.

same as the curve (1). These line profiles are represented by the curves (3) and (4) of Fig. 8. From these experiments, it seems that the line profile may be obtained from electrons passing through the φ-baffle slits but not from scattered electrons.

Let us consider the maximum peak current of the line profile (1) of Fig. 8. As represented by the curve A, the profile obtained with the cone baffle[2] for 1.2 mm dia. Cs^{137} source at the slit position of R-1, indicates the maximum peak current of 2.379 amp., as expected, and the resolution 0.37%. Considering the signification of the fact that the peak current of the line profile is lower by 0.044 amp, than the expected value, the rays selected by the baffle have probably the source effect corresponding to this current deviation. When the spectrometer current is set at 2.379 amp., the rays passing through the φ-baffle will be at the lower radial position than that of the ring slit, corresponding to 0.044 amp. in average. If the spectorometer current is set at the lower value to fall on the ring slit, the rays may be stopped by the Hubert baffle and the available $\Delta\alpha$ may decrease, so that the peak intensity becomes probably extremely small.

To confirm experimentally above considerations, we obtained the line profiles for several R-slit positions with the φ-baffle of 14 plates. For the slit positions of R-2, R-3, R-4, and R-5 the line profiles (5), (6), (7), and (8) are obtained, respectively, as shown in Fig. 8. The difference of curves (7) and (6) yields the line profile A′. The line profile

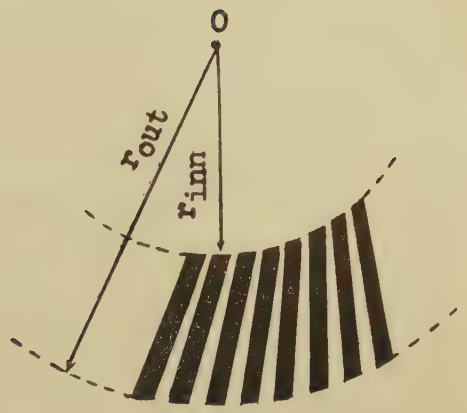

Fig. 6. Section of the baffle perpendicular to the instrument axis.

of this difference will be obtained when the inner baffle R is at the position of R-4 and the outer baffle R' displaced to the R'-(1). The A′ line profile has the maximum peak at the expected spectrometer current i_0, and it is implied that the selected rays have the trajectories running through between R'-(1) and R-(4), at the current i_0. Actually, the numerical calculation shows that the trajectory of the 1420 *gauss cm/amp.*-ray with $\varphi_0 = -40°59'15''$ and emission angle $\alpha_0 = 12°41'$ from the source radius 1 cm, has the lower radial distance by 4.5 mm than that of the point source, at the axial distance of the ring slit. The difference of the rotating angles of these is found to be 17°, and it is hardly negligible.

Thus, it is not unreasonable that the small line profile with 0.5% resolution was obtained, when we used the φ ($= -40°59'15''$) selecting baffle.

Further Investigation

By the experimental analysis, we know now the

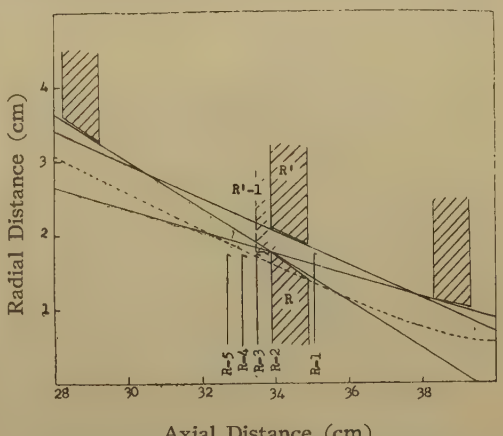

Fig. 7. Ring baffle geometry showing various settings.

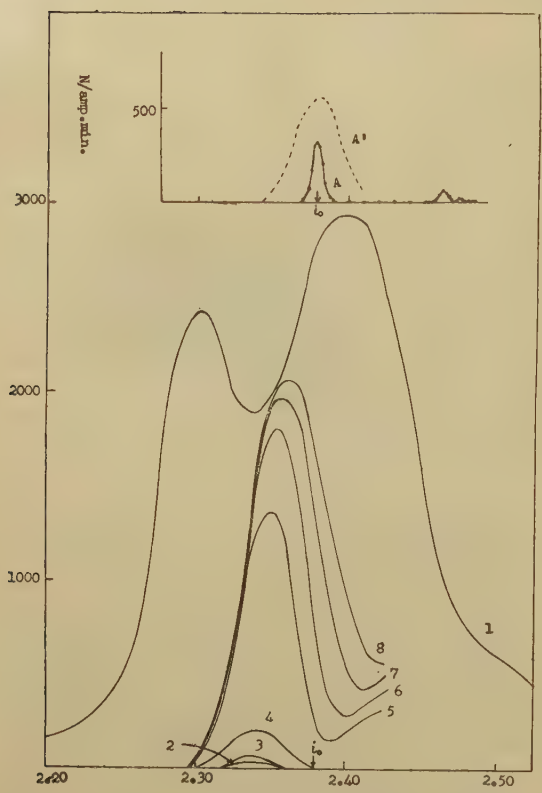

Fig. 8. Experimental line profiles.

fact that the ray with the angle φ, which make $\cos(\varphi+\varphi_{ro})$ vanish, shows some appreciable source effect at the ring slit for the point source. Therefore the question is how we obtain the desired angle.

At the ring slit for the point source y_r is the radial distance of the ray originating from a source point of radius S, and ρ the radial distance of the point source ray. The difference of y_r and ρ, Δy_r, satisfies the next equation;

$$\Delta y_r = \sqrt{\rho_r'^2 + S^2 + 2\rho_r' S\cos\psi_r^*} - \rho \qquad (\psi_r^* = \varphi + \psi_r) \qquad (12)$$

$$= \rho_r'\left[1 + \left\{\frac{S^2}{\rho_r'^2} + 2\frac{S}{\rho_r'}\cos\psi_r^*\right\}\right]^{\frac{1}{2}} - \rho$$

$$= (\rho_r' - \rho) + S\cos\psi_r^* + \frac{1}{2}\frac{S^2}{\rho_r'} - \frac{1}{8}\frac{S^4}{\rho_r'^3} - \frac{1}{2}\frac{S^3}{\rho_r'^2}\cos\psi_r^* - \frac{1}{2}\frac{S^2}{\rho_r'}(\cos\psi_r^*)^2 + \cdots$$

or

$$= (\rho_r' - \rho) + S\cos\psi_r^* + \Delta, \qquad (13)$$

$$\Delta y_r = \left[(\rho_r' - \rho) + \frac{1}{2}\frac{S^2}{\rho_r'} - \frac{1}{8}\frac{S^4}{\rho_r'^3} + \cdots\right] + \left[1 - \frac{1}{2}\frac{S^2}{\rho_r'^2} - \frac{1}{2}\frac{S}{\rho_r'}\cos\psi_r^* + \cdots\right] S\cos\psi_r^*$$

$$= \Delta' + m' S\cos\psi_r^*, \qquad (14)$$

where ρ_r' is the projected distance from the source point to the electron position at the ring slit. According to the numerical calculations, the rotating angle for the finite source radius ($S=1$ cm) is different from that for the point source. And the value of ρ' is found to be appreciably apart at the ring slit from that for the point source. For finding any approximately good functional forms for Δy_r, therefore, it is necessary to calculate the trajectaries of a large number of rays with various initial conditions.

Giving up to find analytically our desired values of φ from Eqs. (3), (4) and (5), we obtained directly these values of angle φ from numerical calculations. To obtain the desired values of angle φ, the next procedure seems to be useful. The source radius, the emisson angle, and the electron momentum being held constant, ρ_r' and ψ_r in Eq. (3) are the functions of φ. Substituting the values for the $\varphi_0 = -40°59'15''$ ray into ρ_r' and ψ_r, the equation

$$y = \left[\rho_r'^2 + S^2 + 2\rho_r' S\cos(\varphi + \psi_r)\right]^{\frac{1}{2}} \qquad (15)$$

involves φ explicitly in $\cos(\varphi+\psi_r)$ only. Then y_r as a function of φ is represented by the dotted curve of Fig. 9. If the value of φ is $-70°17'5''$, y_r estimated from this dotted curve is equal to ρ. By the numerical calculation of the trajectory with this angle, Δy_r is found to be -0.01 cm. When the values for $\varphi_0 = -55°$ ray are substituted into ρ_r' and ψ_r, a similar curve is obtained and, surprisingly, the desired value of φ obtained from this curve is about $-70°$. Thus, when the values of ρ_r' and ψ_r of a ray with any value of angle φ in this region are calculated, one may obtain the desired value of φ approximately. Furthermore, it is interesting to see that the three y_r points corresponding to the $\varphi = -40°59'15''$, $-55°$, and $-70°17'5''$, are lying on the straight line to a good approximation as shown in Fig. 9. As represented by the line S-0.5 of Fig. 9, three points for rays originating from the source radius 0.5 cm tend also to lie on the straight line. Thus if the y_r values of any two rays with different angles φ are obtained, we may find the desired values of angle φ to a better approximation.

Fig. 10 represents the α-focusing property of the rays with the angle $\varphi = -70°17'5''$. These three rays originate from a source point located off the axis at radius 1 cm with emission angle $\alpha = 12°41'$, $14°35'$ and $10°47'$. The position of the α-focusing is not the same for the point source but it deviates by 0.7 cm in axial distance and is somewhat lower in radial distance. However, the spherical aberration coming from the $\Delta\alpha$ is smaller than that for the point source. Then, the position of the ring slit may be chosen at this position. Such values of angle φ that these φ-rays emitted from the source

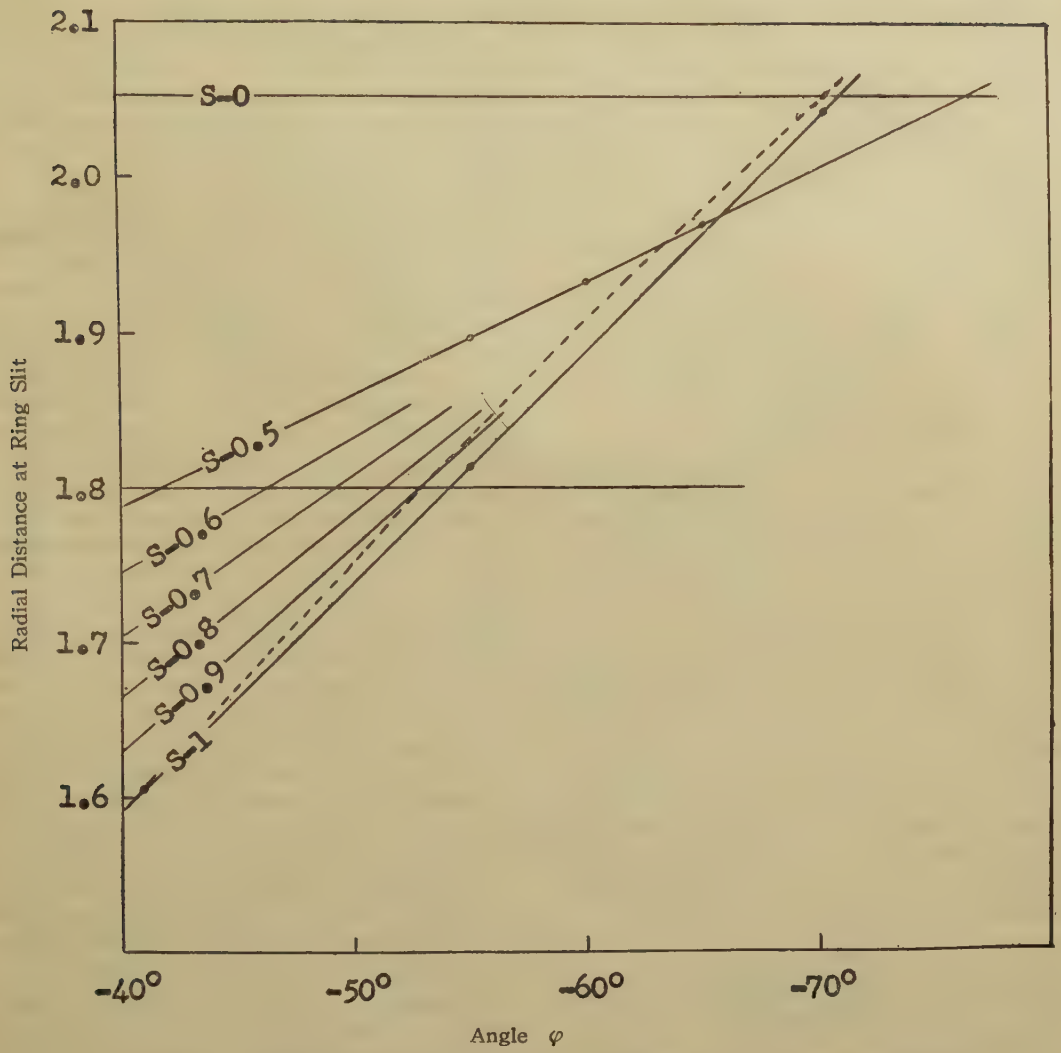

Fig. 9. Calculated y_r-values *vs* φ curves. The desired φ-values are estimated from these to a considerably good approximation.

points at various source radius focus at this position, can be found to a good approximation by the graph smilar to Fig. 9. For source radius 0.5 cm, this angle is found to be $-75°$. If the rays with these angles could be selected, the expected improvement would be obtained.

However, one must face to the difficulties as below in the actual design of this baffle. The slot EFGH, shown in Fig. 11, is a similar one to the slot $A_1A_2C_2C_1$ in Fig. 5. The rays of the desired values of φ and emitted from the source points located from radius 1 cm to 0.5 cm with the emission angle 12°41′, pass through this slit. However, the almost rays with the smaller emission angle than 12°41′ could not pass through it and all the rays with lager emission angle than 12°41′ permitted by this slit have the undesired value of φ. To pass through selectively all the rays with the emission angle between 14°35′ and 10°47′, we must have such a slit ABCD for $S=1$ cm and A′B′C′D′ for $S=0.5$ cm. When we want to utilize all over the source radius from 1 cm to 0.5 cm, we must have a large slit area from ABCD to A′B′C′D′. Such a large slit permits the rays of undesired values of φ and the spread of the rays at the ring slit becomes large. For the possible design of the baffle permitting the rays of the desired values of φ, the baffle slits for the various source radius must lie upon one another.

Therefore, let us consider the focusing of the rays from various source radius at the lower radial distance than the ring slit for the point source. From

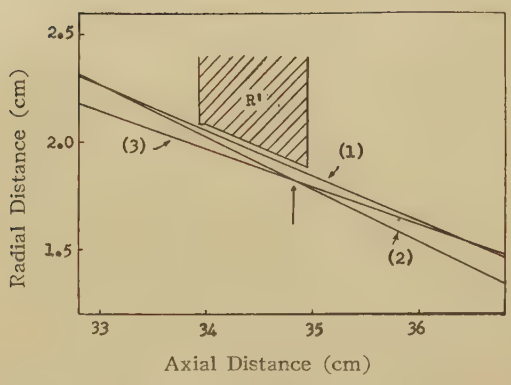

Fig. 10. α-focusing property of the rays of $\varphi = -70°\ 17'\ 5''$.

the curves S-1 and S-0.5 in Fig. 9, the values of φ are found to be $-54°$ for $S=1$ cm and $-41°40'$ for $S=0.5$cm, if y_r is 1.8 cm. Similarly, for the other source radius, it can be assumed that the φ-dependence of the radial distance y_r will be represented by the straight line in these φ-region.

The values of y_r at $\varphi=-40°$ and the tangential values are interpolated by those of three straight lines, S-0, S-1 and S-0.5 in Fig. 9. Then, the straight line for any arbitrary source radius are obtained approximately. The straight lines denoted by S-0.6, S-0.7, S-0.8 and S-0.9 are drawn by this approximate method for source radius 0.6, 0.7, 0.8 and 0.9 cm, respectively. By the graph in Fig. 9, the values of φ at $y_r=1.8$ cm are found. These values are shown in Table Ⅱ.

Table Ⅱ

S cm	k gauss cm/amp.	α	φ	y_r cm
1.0	1420	12°41′	−54°	1.798 8462
0.9	〃	〃	−53°	(1.8)
0.8	〃	〃	−51°30′	1.800 9645
0.7	〃	〃	−49°20′	(1.8)
0.6	〃	〃	−46°20′	(1.8)
0.5	〃	〃	−41°40′	(1.8)

The numerical calculations show that the radial distances of the rays with these values of φ, are 1.8 cm to a good approximation at z_r. The ray originating from each source radius with a certain emission angle other than 12°41′ may have the maximum radial distance at z_r, but this emission angle and its maximum radial distance may be not so far from those of the ray with the emission angle 12°41′. For the source radius 1 cm, the ray with the emission angle ∼12°46′ has the maximum radial distance ∼1.7990 cm at z_r. As seen in Table Ⅱ, if the radial distance of the focusing is lower than that for the point source (∼2.0536 cm), the rays originating from the larger source radius must have the smaller values of φ to focus at the same radial position, in the region of these values of φ. Thus, the slots of the baffle for various source radius tend to approach each other. The better condition of overlapping of these slots may be found for other values of φ, but if the values of φ shown in Table Ⅱ are adopted it does not seem to deviate appreciably from optimum value. To examine the system of the baffle slit permitting the rays of the angle φ in Table Ⅱ, the slots for source radius 1 cm, 0.9 cm, and 0.8 cm are shown in Fig. 12. These slots, at the axial distance 12 cm from the source, have the large common part of area. Therefore, it is likely to decrease largely the stray passage of undesired rays. When the baffle is set from such position to the neighbourhood of the source, the expected spread of the line profile may be obtained. However, in the neighbourhood of the source, these slots for various source radius become to be apart from each other. To keep the available source area a half, the next neighbouring slits must have the shaded area indicated in Fig. 12. From the configuration of these slits, it is evident that the setting of the baffle at the axial distance 4 cm is difficult, if the source radius from 1 cm to 0.8 cm is utilized. When the source radius is utilized from 1 cm to 0.8 cm, the baffle can not be set within the axial distance 6 cm. If there is no baffle near the source, it is necessary to set the baffle at the position far from the source, so as to hold $X_m=3°$. However, at a too far distance from the source, the slit width becomes large, so that the neighbouring slits overlap each other.

As a result, the available source width is found to be only 0.2 cm at $S=1.0$ cm, for S-focus suggested by Beard.[5] Thus, in actual design, we could not obtain the available source radial width so large as expected.

Conclusion

The S-focus, that could be expected theoretically to be capable of the considerable improvement, contains some difficulties as described. Although the elaborate calculation to find the optimum φ, stray passage of the undesired φ-rays and difficult fabrication are not so important, yet it is important that available source width must be small to diminish the loss factor. Thus it is concluded that the S-focus, including first order α-focus, must be compared quantitatively with the complete α-focus, including somewhat S-focus, to find the best focus mode depending on the φ-slection.

(Laboratory of Physics, Received Aug. 30, 1958)

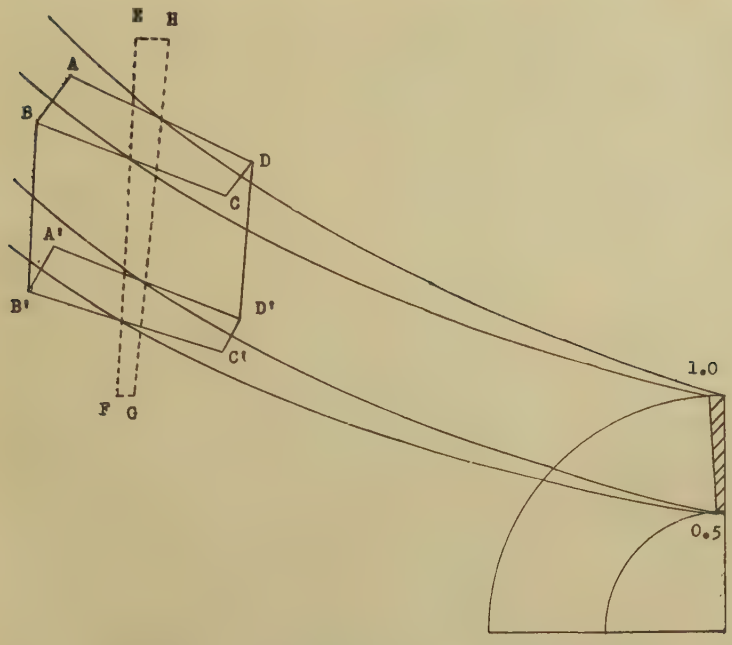

Fig. 11. Slot geometry for the rays focusing at the radial distance of~2.05cm.

References

1) P. Hubert, *Ann. de Phys.* **8**, 662 (1953)
2) K. Takazawa, M. Higuchi, K. Ohira and H. Matsui, *Sci. Rep. Hyogo Univ. Agric.* Vol. **3**, No. 1, Ser: Natur. Sci., p. 9 (1957)
3) J. A. Jungerman and D. B. Beard, *Rev. Sci. Instr.* **27**, 56 (1956)
4) J. A. Jungerman and D. B. Beard *Rev. Sci. Instr.* **27**, 650 (1956)
5) D. B. Beard, *Rev. Sci. Instr.* **28**, 19 (1957)
6) J. M. Keller, E. Koenigsberg and A. Paskin, *Rev. Sci. Instr.* **21**, 713 (1950)

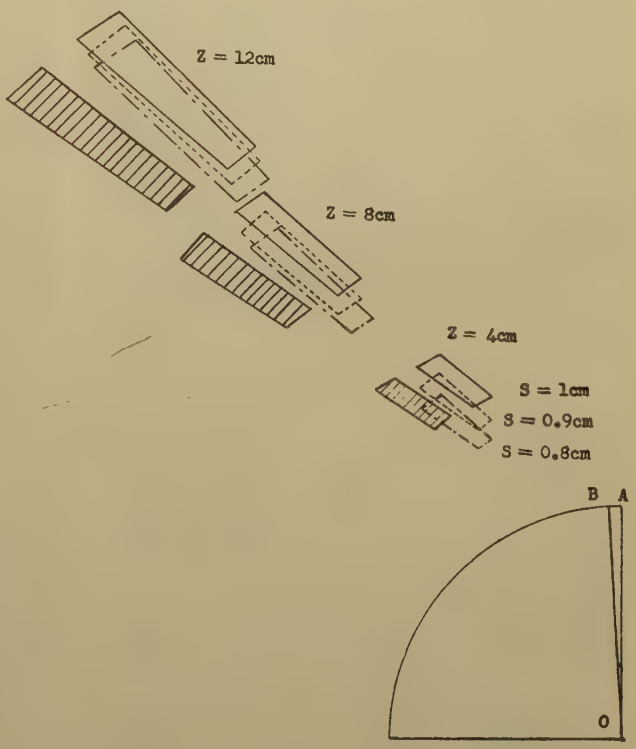

Fig. 12. Slot geometry for the rays focusing at the radial distance of~1.8cm.

SOME NEW SPECIES OF THE GENUS *PTEROSTICHUS* FROM WESTERN JAPAN

(Coleoptera: Harpalidae)

Hiroshi Ishida

In this paper, the author describes four new species of the genus *Pterostichus* Bonelli, 1810, from Honshû, Japan, which are belonging to the *sphodriformis* group (including *sphodriformis* H. W. Bates, 1873[1]; *pachinus* H. W. Bates, 1883[2]; *mucronatus* Straneo, 1955[3]; *abaciformis* Straneo, 1955[4]; *kyushuensis* Habu, 1955[5], and *shiibanus* Habu, 1958[6]). But the subgeneric reference to *Pterostichus*, s. str. is somewhat doubtful and therefore, further study will be desired.

Before going further, the author wishes to express his hearty thanks to Prof. Takehiko Nakane, the Saikyo University, Kyoto, for his constant helps and kind suggestions and to Prof. Seizaburo Hasegawa and Prof. Michiyoshi Takezaki, the Hyogo Agricultural College, Kakogawa, for their kind helps in photographing of specimens. He also greatly indebted to the following gentlemen, for their kind aids to give or loan their valuable specimens: Messrs. Kunio Fujita, Mitsuo Goto, Masao Hayashi, Teitaro Horio, Yoshikazu Ikutani, Takashi Kishii, Isaburo Kono, Kosaku Masida, Akira Nobuchi, Masafumi Ohkura, Kazuo Tanaka, Masahiko Yoshikawa, and member of the Natural Science Club of the Masuda Industrial High School, Masuda, Shimane Pref.

Pterostichus (s. str.) *yoshikawai* sp. nov.

Nom. Jap.: Yoshikawa-naga-gomimushi.
(Figs. 1, 6, 10, 14)

1958 *Pterostichus* (s. str.) *yoshikawai* Ishida,
Akitu, Kyoto, 71:19 (in litt).

Length: 13.0 mm.; width: 4.3 mm.

Black, shiny, not iridescent; palpi and tarsi reddish brown, but apex of palpi paler; antennae and rests of legs dark brownish black; underside black.

Head normal, rather convex; surface very minutely punctate; microsculpture faint, forming almost isodiametric meshes; eyes moderate, convex; temporae tumid, shorter than eyes; posterior supraorbital setae almost on the level of posterior margin of eyes; neck strongly constricted, rather flat; frontal furrows rather deep, subparallel each other; antennae long, 2nd segment with one seta on ventral side, and basal three segments glabrous; apex of palpi truncate; tooth of mentum bifid.

Pronotum cordiform, very strongly constricted behind, rather convex, widest near apical one-third, and wider than long; surface almost smooth, but inner sides of basal foveae except middle rugose with several large punctures; microsculpture faint, forming transverse meshes; apical margin sinuate, very weakly bordered; anterior angles scarcely protrudent, rounded; lateral channel clearly punctulate, near apex depressed and not explanate; lateral margin near posterior angles denticulate or sinuate; posterior angles acute, almost rectangular; base sinuate, narrower than apex, and bordered near posterior angles; basal margin at middle with very weak vertical wrinkles; anterior setae at about two-fifths from apex; posterior setae slightly before posterior angles; median line distinct, reaching basal margin; basal foveae rather deep, linear, weakly rugose-punctate, and subparallel each other.

Wings apterous. Elytra shiny, not iridescent, convex, elongate-ovate, and widest near apical one-third; each elytron fused each other at suture; surface smooth; microsculpture forming almost isodiametric meshes; basal border scarcely oblique, adjoining lateral margin forming obtuse angle; shoulder rounded; lateral channel not widened at apex; apical sinuation slight; apex rather angulate; striae strongly impressed, impunctate; scutellary striole oblique, short, present on 1st interstice; interstices convex, 3rd interstice with four dorsal pores at about basal one-fourth, two-fifths,

1) Trans. ent. Soc. London, 1873: 289-290; type: Hiogo.
2) Ibid., 1883:245; type: Junsai.
3) Ann. Mus. Civ. Stor. Nat. Genova, 68:93-94, figs. 5, 17, 24; type: M. Yatsu (1700-1900m.), Shinano.
4) Ibid., 97-98, fig. 7; type: Simasima, Shinano.
5) Bull. nat. Inst. agric. Sci. Japan, (C) 5:152-155, figs. 5, 8; type: Hikosan, die Provinz Fukuoka, Kyûshû.
6) Kontyû, Tokyo, 26(2):70-72, figs. 2, 5; type: Shiiba, Miyazaki Pref., Central Kyûshû.

middle, and three-fourths, and first one adjoining 3rd stria and remaining ones adjoining 2nd stria; umbilicate pores 17 in number, weakly interrupted at middle.

Meso- and metatarsi with basal three segments sulcate at outer side; 5th segment of all tarsi glabrous beneath.

Underside almost smooth, but proepisterna strongly, mesosternum sparsely, and basal half of mesepisterna rather strongly punctate; prosternal process with longitudinal furrow in middle, apex unbordered, glabrous, and apical margin rounded; metepisterna slightly wider than long, sulcate at front side; anal sternite (Fig. 6) in male, strongly excavated at apical half and weakly keeled longitudinally in middle, and apical margin sinuate, reflexed at middle, with one marginal seta on each side.

Aedeagus (Figs. 10, 14) reddish brown, slender, curving more than rectangular; right ventral side with weak tumor; membraneous part long; apical lamella triangular, small, and apex rather pointed; right paramere short, narrowed at middle, and apex rather rounded; left paramere quadrate, strongly excavated in middle.

Holotype, male (Fig. 1), Mt. Ohdaigahara, Nara Pref., Honshû, 22. VI. 1957, Masahiko Yoshikawa leg., in T. Nakane's collection.

This species resembles *Pterostichus* (*Paralianoe*) *takahashii* Ishida, 1958 (Entom. Rev. Japan, Osaka, 9(1):6, figs. 7, 8, 16, 22, 28; 9(2):33-34) from the same locality, but at once distinguished from the latter on the following points: Strongly shiny, convex body, pronotum with only one anterior seta, smooth surface of tarsi, unbordered prosternal process, and especially shape of anal sternite in male and aedeagus, etc., and the name is dedicated to the collector, Mr. Masahiko Yoshikawa, Fujiidera-chô, Osaka Pref.

Pterostichus (s. str.) *masidai* sp. nov.

Nom. Jap.: Masida-naga-gomimushi.
(Figs. 2, 7, 11, 15)

Length: 14.7 mm.; width: 4.8 mm.

Black, shiny, not iridescent; palpi reddish brown, but apex paler; antennae and tarsi dark reddish brown, rests of legs much darker: underside dark brownish black.

Head normal, rather convex; surface minutely punctate; microsculpture faint, forming almost isodiametric meshes; eyes moderate, convex; temporae tumid, shorter than eyes; posterior supraorbital setae almost on the level of posterior margin of eyes; neck strongly constricted, rather convex; frontal furrows rather shallow, subparallel each other; antennae long, 2nd segment with one seta on ventral side, and basal three segments glabrous; apex of palpi scarcely truncate; tooth of mentum bifid.

Pronotum cordiform, rather strongly constricted behind, rather convex, widest near apical one-third, and almost as wide as long; surface almost smooth, except area between basal foveae and lateral margins and inner sides of basal foveae except middle strongly rugose-punctate; microsculpture faint, forming transverse meshes; apical margin sinuate, very weakly bordered; anterior angles weakly protrudent, rounded; lateral channel weakly punctulate, near apex depressed, almost smooth, and not explanate; lateral margin near posterior angles denticulate; posterior angles acute, almost rectangular; base sinuate, narrower than apex, and bordered near posterior angles; basal margin at middle with strong and short vertical wrinkles; anterior setae at about one-third from apex; posterior setae slightly before posterior angles, median line distinct, not reaching both margins; basal foveae rather deep, linear, rugose-punctate, and subparallel each other.

Wings apterous. Elytra shiny, not iridescent, convex, elongate-ovate, and widest near apical one-third; each elytron not fused each other at suture; surface smooth; microsculpture forming almost isodiametric meshes; basal border sinuate, adjoining lateral margin forming obtuse angle; shoulder rounded; lateral channel not widened at apex; apical sinuation rather slight; apex almost rectangular; striae strongly impressed, impunctate; scutellary striole oblique, rather long, present on 1st interstice; interstices convex, 3rd interstice with three dorsal pores at about basal one-fourth, middle, and three-fourths, and first one adjoining 3rd stria and remaining ones adjoining 2nd stria; umbilicate pores 15 or 20 in number, weakly interrupted at middle.

Meso- and metatarsi with basal three segments sulcate at outer side; 5th segment of all tarsi glabrous beneath.

Underside almost smooth, but proepisterna, mesosternum, basal half of mesepisterna rather strongly punctate, metepisterna and basal two lateral abdominal sternites sparsely punctate; prosternal process rather wide, weakly excavated in middle, and bordered at apex, apical margin almost straight, glabrous; metepisterna slightly wider than long, sulcate at front side; anal sternite (Fig. 7) in male, weakly excavated at apical half and very weakly keeled longitudinally in middle, apical margin sinuate, reflexed at middle, with one marginal seta on each side.

Aedeagus (Figs. 11, 15) dark brownish black, rather robust, curving more than rectangular; right ventral side with slight tumor; membraneous part long and wide; apical lamella small, triangular, and apex rather pointed; right paramere short,

narrowed at middle, and apex rather rounded; left paramere quadrate, strongly excavated in middle.

Holotype, male (Fig. 2), Mt. Kammuri, Shimane Pref., Western Honshû, 26. Ⅶ. 1953, Kosaku Masida leg., in the author's collection.

This species is closely allied to *Pterostichus* (s. str.) *yoshikawai* sp. nov., but distinguished from the latter on the following points: Larger body, shape and punctuation of pronotum, unfused elytron, number of dorsal pores, rectangular apex of elytra, prosternal process, punctuation of abdomen, anal sternite in male, and aedeagus, etc. and these two new species are characteristic in the *sphodriformis* group on the following points: Much smaller, very convex body, position of scutellary striole, and anal sternite in male, etc., and the name is dedicated to the collector, Mr. Kosaku Masida, the Masuda Industrial High School.

Pteristichus (s. str.) *esakii* sp. nov.

Nom. Jap.: Esaki-naga-gomimushi.
(Figs. 3, 8, 12, 16)

Length: 18.0 mm.; width: 6.2 mm.

Black, shiny, not iridescent; palpi reddish brown, but apex much paler; antennae, tibiae, and tarsi dark brownish black, rests of legs black; underside black.

Head large, rather flat; surface very minutely punctate; microsculpture faint, forming almost isodiametric meshes; eyes rather small, rather flat; temporae tumid, shorter than eyes; neck weakly constricted, convex; frontal furrows rather shallow, subparallel each other; antennae long, 2nd segment with one seta on ventral side, and basal three segments glabrous; apex of palpi scarcely truncate; tooth of mentum bifid.

Pronotum cordiform, very strongly constricted behind, rather flat, widest near apical one-fourth, and wider than long; surface almost smooth, but several punctures near basal foveae; microsculpture faint, forming transverse meshes; apical margin sinuate, very weakly bordered; anterior angles protrudent, rounded; lateral channel clearly punctulate, near apex depressed and explanate; lateral margin near posterior angles scarcely denticulate; posterior angles obtuse, narrowly rounded; base strongly sinuate, narrower than apex, and bordered near posterior angles; anterior setae at apical one-fourth; posterior setae at slightly before posterior angles; median line distinct, not reaching both margins; basal foveae rather deep, linear, smooth, and divergent before and subparallel to lateral margin.

Wings apterous. Elytra shiny, not iridescent, flat, elongate elliptic, and widest near middle; surface impunctate except outer interstices; microsculpture forming almost isodiametric meshes; basal border scarcely oblique, adjoining lateral margin forming obtuse angle; shoulder rounded; lateral channel not widened at apex; apical sinuation rather distinct; apex rather rounded; striae deep, very faintly punctulate; scutellary striole very short or absent, if present, on 2nd interstice; interstices flat, 3rd interstice with three dorsal pores at about basal one-fourth, middle, and three-fourths, and first one adjoining 3rd stria and remaining ones adjoining 2nd stria; umbilicate pores interrupted at middle, 17 in number.

Meso- and metatarsi with basal three segments sulcate at outer side; 5th segment of all tarsi glabrous beneath.

Underside almost smooth, but mesosternum sparsely and basal parts of mesepisterna strongly punctate, lateral parts of basal one abdominal sternite punctate at basal half; prosternal process with longitudinal furrow in middle, apex weakly bordered, glabrous, and apical margin rounded; metepisterna almost as wide as long, sulcate at front side; anal sternite (Fig. 8) in male, strongly excavated at apical half and keeled longitudinally and then swollen triangularly at apical margin, apical margin sinuate, reflexed at middle with one marginal seta on each side.

Aedeagus (Figs. 12, 16) reddish brown, slender, long, curving more than rectangular; right ventral side with very long and large tumor, membraneous part short; apical lamella small, almost quadrate, and apex rounded and not twisted; right paramere short, narrowed at middle, slightly curved, and apex rounded; left paramere quadrate, strongly excavated in middle.

Holotype, male (Fig. 3), Hikimi to Hiromi, foot of Mt. Gori, Hikimi-chô (formerly Hikimi-kami-mura), Mino-gun, Shimane Pref., Western Honshû, 26. Ⅶ. 1957, Kiyoshi Inoki leg., in the author's collection.

This species is allied to *Pterostichus* (s. str.) *sphodriformis* H. W. Bates, 1873 (Figs. 5, 9, 13, 17), but differed from the latter on the following points: Darker legs, protrudent anterior angles, bordered prosternal process, and especially anal sternite in male and aedeagus, etc. and it was found under the mosses with *Broscosoma dönitzi* (Harold, 1881), subsp., and the name is dedicated to late Prof. Dr. Teiso Esaki, the Kyushu University, Fukuoka, with the deepest sorrow.

Pterostichus (s. str.) *tsurugaensis* sp. nov.

Nom. Jap.: Tsuruga-naga-gomimushi.
(Fig. 4)

Length: 20.0 mm.; width: 6.5 mm.

Black, shiny except elytra; antennae, palpi, legs dark reddish brown, but apex of palpi paler and femora much darker; underside black.

Head large, moderately convex; surface sparsely and very minutely punctate; microsculpture faint, forming almost isodiametric meshes; eyes moderate, rather convex; temporae tumid, rather shorter than eyes; posterior supraorbital setae slightly behind the level of posterior margin of eyes; neck constricted, convex; frontal furrows rather deep, broad, and divergent behind; antennae long, 2nd segment with one or two setae on ventral side, 3rd segment slightly longer than 1st, and three basal segments glabrous; apex of palpi truncate; tooth of mentum bifid.

Pronotum cordiform, strongly constricted behind, rather convex, widest near apical one-fourth, and wider than long; surface impunctate; microsculpture faint, forming transverse meshes; apical margin sinuate, slightly bordered; anterior angles protrudent, rounded; lateral channel almost smooth, near apex widely explanate, and less depressed than in allied species; lateral margin near posterior angles weakly denticulate; posterior angles very narrowly rounded, almost rectangular; base almost as wide as apex, bordered near posterior angles, and slightly sinuate; anterior setae at apical one-fourth; posterior setae rather before posterior angles; median line distinct, not reaching both margins; basal foveae rather deep, linear, smooth, and subparallel each other.

Wings apterous. Elytra opake, flat, elongate elliptic, and widest near middle; each elytron fused with each other at suture; microsculpture forming almost isodiametric meshes; basal border scarcely oblique, adjoining lateral margin forming acute angle; shoulder rounded; lateral channel not explanate at apex; apical sinuation rather slight; apex rounded; striae shallow; impunctate; scutellary striole rather long, present on 2nd interstice; interstices flat, 3rd interstice with four dorsal pores at about basal one-fourth, middle, two-thirds, and three-fourths, and first one adjoining 3rd stria and remaining ones adjoining 2nd stria; umbilicate pores clearly interrupted at middle, 18 or 21 in number.

Metafemora unusually long, metatrochanters clearly shorter than half of metafemur; mesc- and metatarsi with basal three segments sulcate at outer side; 5th segment of all tarsi glabrous beneath.

Underside almost smooth, but basal half of metepisterna sparsely punctate, lateral parts of 1st abdominal sternite rather strongly punctate at basal half and 2nd sternite punctate sparsely; metepisterna almost as long as wide, sulcate at front side; prosternal process widely but weakly bordered at apex, apical margin almost straight, glabrous, and furrowed longitudinally in middle, but slightly behind the coxae, the furrow forked and shallower; anal sternite in female, somewhat depressed at apical half, along the apical margin with strong wrinkles, apical margin almost straight at apex, with two marginal setae on each side.

Holotype, female (Fig. 4), Tsuruga, Fukui Pref., Honshû, 6. Ⅷ. 1956, Takehiko Nakane leg., in his collection.

This species is allied to female with opake elytra of *Pterostichus* (s. str.) *sphodriformis* H. W. Bates, 1873, from lower mountains of Kinki districts, but differed from the latter on the following points: Broader and deeper frontal furrows, shape of pronotum, especially less depressed anterior angles, shallower stria of elytra, clearly interrupted umbilicate pores, rounded apex of elytra, longer metafemora, prosternal process, and punctuation of underside, etc., and it was found at seashore near Tsuruga, but it might be carried away from the neighbouring mountainous districts owing to inundation of river.

(Entomological Laboratory of Kakogawa Branch, Received Aug. 23, 1958)

Postscript

In course of the printing of this paper, the author has received four specimens of *Pterostichus masidai* sp. nov. by the courtesy of Mr. Kosaku Masida, and therefore, he designates them as allotype and paratypes and gives supplementary notes.

Allotype: Length: 14.8 mm.; width: 5.0 mm.

Almost same as the holotype, but differed as follows: Tarsi reddish brown; punctuation of pronotum less densely near basal foveae; elytra with silky gloss; scutellary striole present on 2nd interstice; apex of elytra rather rounded; umbilicate pores clearly interrupted at middle; underside black, punctuation less densely; anal sternite at apical half depressed, apical margin almost straight, with two marginal setae on each side.

Paratypes: Length: 14.2–14.7 mm.; width: 4.3–4.8 mm.

Almost same as precedings, but position of scutellary striole is uncertain, present on either 1st or 2nd interstice; apex of elytra more or less rounded; umbilicate pores weakly or clearly interrupted; punctuation somewhat variable, rather sparsely distributed; tarsi reddish brown, in certain cases antennae also reddish brown.

Allotype, female, Mt. Kammuri to Mikazura, 22. Ⅶ. 1958, Hisao Fukuhara leg., in T. Nakane's collection; paratypes, 2 males and 1 female, Mt. Kammuri, 21. Ⅶ. 1958, Takeshi Kodama & Takashi Watanabe leg., in K. Tanaka's and the author's collection.

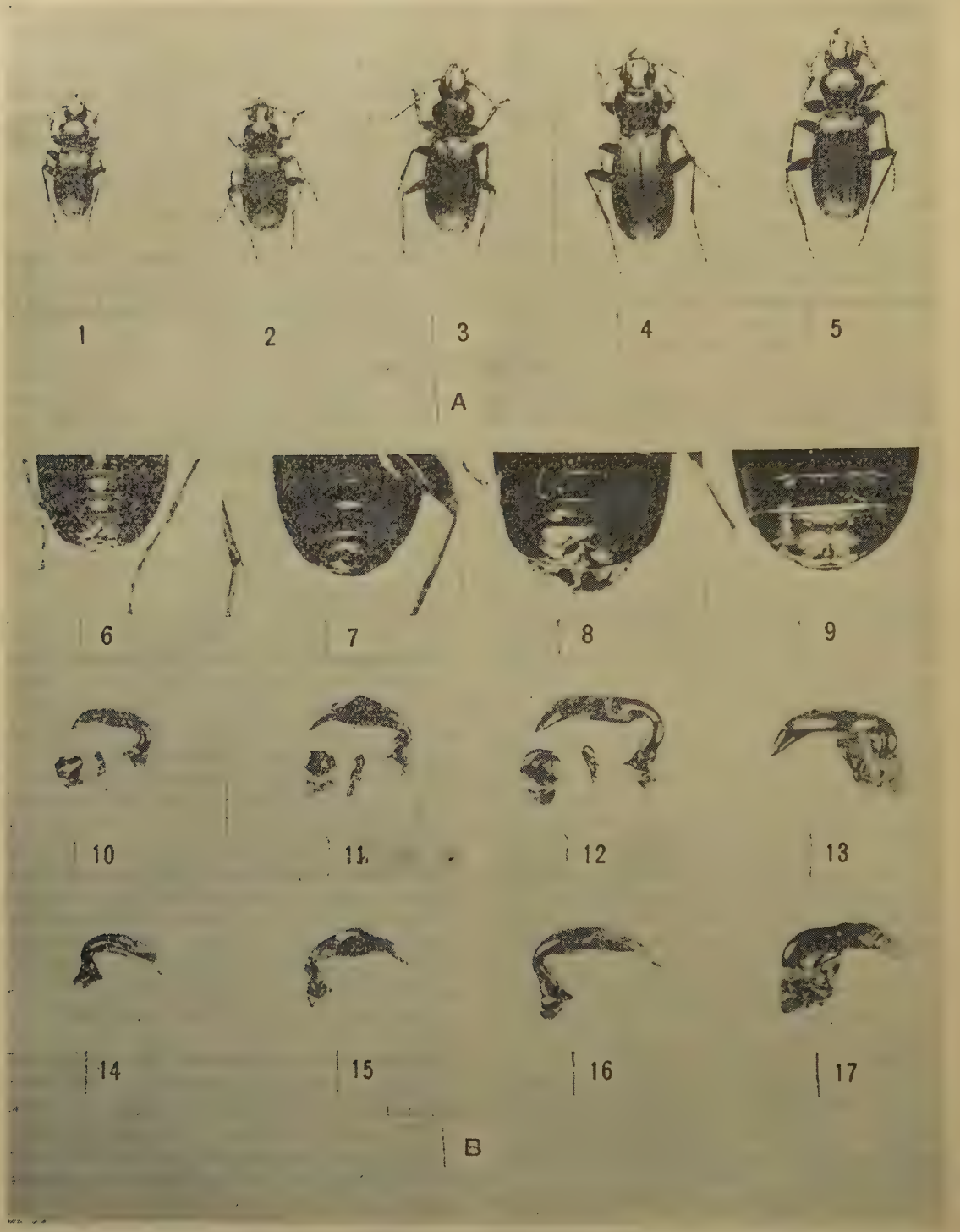

Explanation of figures.

Figs. 1-5: Dorsal view of insect (Scale A:1 unit equals 0.5 mm.).
Figs. 6-9: Anal sternite in male (Scale B:1 unit equals ca. 0.17 mm.).
Figs. 10-13: Right lateral side of aedeagus (Scale B: 1 unit equals ca. 0.15 mm.).
Figs. 14-17: Left lateral side of aedeagus (Same as above).
Figs. 1, 6, 10, 14: *Pterostichus* (s. str.) *yoshikawai* sp. nov. (Holotype).
Figs. 2, 7, 11, 15: *Pterostichus* (s. str.) *masidai* sp. nov. (Holotype).
Figs. 3, 8, 12, 16: *Pterostichus* (s. str.) *esakii* sp. nnv. (Holotype).
Fig. 4: *Pterostichus* (s. str.) *tsurugaensis* sp. nov. (Holotype).
Figs. 5, 9, 13, 17: *Pterostichus* (s. str.) *sphodriformis* H. W. Bates, 1873 (From Ashû, Miyama-chô, Kita-Kuwada-gun, Kyôto Pref.).

THE CATALOGUE OF THE JAPANESE TIPULIDAE, WITH THE KEYS TO THE GENERA AND SUBGENERA (Diptera)

IV. LIMONIINAE, TRIBE PEDICIINI

Hiroshi Ishida

The three preceding parts under this general title were published in the *KENKYU SHUROKU* (*Annual Reports of the Hyogo Agricultural College*), No. 4 (1954), pp. 106-135, 1955; No. 5 (1955), pp. 59-77, 1956, and No. 6 (1956), pp. 122-149, 1957. At this time the author gives a catalogue and keys of the tribe Pediciini of the subfamily Limoniinae, but the remaining tribes will be published in the following issue of this journal.

The author wishes to express his cordial gratitudes and appreciation to Prof. Dr. Charles P. Alexander, the University of Massachusetts, Amherst, Mass., U. S. A., for his continued aid and encouragement.

The abbreviations used in this part are the same with those of Part III (See, p. 122).

Tribe **PEDICIINI**

1933 *Pediciini* Alex., PJS, 50: 145.
1942 *Pediciini* Alex., Bull. Conn. geol. nat. Hist. Surv., 64: 342-3.

Key to Genera

1. Wings with membrane covered with abundant macrotrichia ····· **Ula**
   Wings with cells glabrous ····· 2
2. Eyes glabrous ····· **Nipponomyia**
   Eyes hairy ····· 3
3. Antennae 12-segmented, supernumerary crossveins in cells R_3, R_4, M_1, and M. ····· **Heterangaeus**
   Antennae 13-segmented or more ····· 4
4. Size large (wing, ♂, usually over 7 mm.; in most cases much larger); antennae with 14 or 16 segments; wings with usually patterned with darker, either as a costal shading or else spotted and marbled; no supernumerary crossvein in cell R_1 ····· **Pedicia**
   Size smaller (wing, ♂, under 7 mm.; where larger, with a supernumerary crossvein in cell R_1); antennae with either 13 or 15 segments; wings immaculate, except for the stigmal darkening ····· **Dicranota**

Genus **PEDICIA** Latreille, 1809

1809 *Pedicia* Latr., Hist. Nat. Crust. et Ins., 4: 255, type: *Tipula rivosa* L.
1916 *Daimiotipula* Mats., Thous. Ins. Jap., Add. 2: 463-4, type: *Daimiotipula daimio* Mats.
1934 *Pedicia* Kariya, PJS, 53: 302-4 (Key to Japanese spp.).

Key to Subgenera

1. Size very large (wing, 20 mm. or more); wings with a dark pattern that is arranged as a triangle, including broad costal and cubital seams that are connected across the very oblique cord; maxillary palpi with terminal segment elongate ····· **Pedicia,** s. str.
   Size smaller (wing, under 18 mm., usually under 15 mm.); wings never with a dark pattern distributed as above described; cord transverse or nearly so; maxillary palpi with terminal segment short ····· 2
2. Wings with a supernumerary crossvein in cell *M* ····· **Nasiternella**
   No supernumerary crossvein in cell *M* of wings ····· **Tricyphona**

Subgenus **PEDICIA,** s. str.

Pedicia (Pedicia) brachycera Alexander, 1933
1933 *P. brachycera* Alex., PJS, 50:145-6, pl. 1, f. 12 (w); pl. 3, f. 40 (♀ ant), type: Shiroumadake, Japanese Alps.
Distribution: **JAPAN** (Honshu).

Pedicia (Pedicia) cubitalis Alexander, 1933
1933 *P.* (*Tricyphona*) *cubitalis* Alex., PJS, 51: 396-8, pl. 1, f. 16 (w), type: Mt. Kurobegoro, Echiu.
Distribution: **JAPAN** (Honshu).

Pedicia (Pedicia) daimio (Matsumura, 1916)
1916 *Daimiotipula daimio* Mats., Thous. Ins. Jap., Add. 2: 462-3, pl. 25, f. 5 (whole ♀), type: Sapporo.

1924 *P. daimio* Alex., PJS, 24:568-9 (♂ description).
1933 *P. daimio* Alex., PJS, 50:146, pl. 3, f. 39 (♀ ant).
1934 *P. daimio* Kariya, PJS, 53:303.
1950 *P. daimio* Esaki, Icon. Ins. Jap., ed. 2:1520, f. 4359.
Distribution: **JAPAN** (Hokkaido).

Pedicia (Pedicia) gaudens (Alexander, 1924)
1924 *Tricyphona gaudens* Alex., AESA, 17:440-1, type: Kyoto.
1953 *P. (P.) gaudens* Alex., PJS, 82:58.
Distribution: **JAPAN** (Honshu).

Pedicia (Pedicia) gifuensis Kariya, 1934
subsp. **gifuensis** Kariya, 1934
1934 *P. gifuensis* Kariya, PJS, 53:304, 305-6, pl. 1, f. 2 (w); f. 6 (hyp); f. 7 (♀ ant); f. 8 (ovip), type: Mt. Kinkwa, Gifu; Pref. Iwate.
1936 *Daimiotipula daimio* Horie, Kansai Konchû Zasshi, 4:47, f. (nec Mats., 1916).
1940 *P. daimia* (sic) Saito, Ent. World, 8:384 (nec Mats., 1916).
1950 *P. gifuensis* Tokunaga, Icon. Ins. Jap., ed. 2:1520, f. 4360.
Distribution: **JAPAN** (Hokkaido; Honshu; Kyushu).

subsp. **sawadai** Kariya, 1934
1934 *P. gifuensis sawadai* Kariya, PJS, 53:306-7, pl. 1, f. 3 (w), type: Gora, Hakone.
Distribution: **JAPAN** (Honshu).

Pedicia (Pedicia) grandior (Alexander, 1923)
1923 *Tricyphona grandior* Alex., AESA, 16:69-70, type: Mt. Hakuba, Shinano.
1950 *Tricyphona grandior* Esaki, Icon. Ins. Jap., ed. 2:1520, f. 4361.
1953 *P. (P.) grandior* Alex., PJS, 82:58-9, pl. 2, f. 15 (hyp).
Distribution: **JAPAN** (Honshu; Kyushu).

Pedicia (Pedicia) issikiella Alexander, 1953
1953 *P. (P.) issikiella* Alex., PJS, 82:57-9, pl. 2, f. 14 (hyp), type: Mt. Tsurugi, Minokosi to Nagoro, Awa; Mt. Ishizuchi, Iyo; Mt. Saragamine, Iyo.
Distribution: **JAPAN** (Shikoku).

Pedicia (Pedicia) nawai Kariya, 1934
1934 *P. nawai* Kariya, PJS, 53:304-5, pl. 1, f. 1 (w); f. 5 (hyp), type: Mt. Ontake, Hida.
Distribution: **JAPAN** (Honshu).

Pedicia (Pedicia) subtransversa Alexander, 1933
1933 *P. subtransversa* Alex., PJS, 50:146-7, pl. 1, f. 13 (w); pl. 3, f. 41 (hyp), type: Shirouma-dake, Japanese Alps.
Distribution: **JAPAN** (Honshu); **N. KOREA.**

Subgenus **TRICYPHONA** Zetterstedt, 1838

1838 *Tricyphona* Zett., Ins. Lapponica, Dipt., 851, type: *Limonia immaculata* Mg.
1856 *Amalopis* Haliday, in Walker's Ins. Brittanica, Dipt., 3, Add., p. xv, type: *Limnobia occulta* Mg.
1856 *Bophrosia* Rondani, Prodr., 1:183, type: *Limnobia immaculata* Mg.
1860 *Crunobia* Kolenati, Wien. ent. Monatschr., 4:391, type: *Crunobia schineri* Kol.
1936 *Olecranopelma* Enderlein, Tierwelt Mitteleur., 6, iii Teil, 2 Lief., XVI:23, type: *Limonia transversa* Mg.

Pedicia (Tricyphona) confluens (Alexander, 1922)
1922 *T. confluens* Alex., IIM, 10:186-7, type: Gifu.
Distribution: **JAPAN** (Honshu).

Pedicia (Tricyphona) fimbriatula Alexander, 1953
1953 *P. (T.) fimbriatula* Alex., PJS, 82:59-61, pl. 2, f. 13 (hyp); f. 16 (w), type: Mt. Tsurugi, Minokosi to Nagoro, Awa.
Distribution: **JAPAN** (Shikoku).

Pedicia (Tricyphona) insulana (Alexander, 1913)
1913 *T. insulana* Alex., Can. Ent., 45:317, 319-20, pl. 4, f. 3 (w), type: Tokyo.
Distribution: **JAPAN** (Honshu; Shikoku; Kyushu).

Pedicia (Tricyphona) kirishimensis (Alexander, 1928)
1928 *T. kirishimensis* Alex., PJS, 35:474-5, pl. 1, f. 6 (w), type: Mt. Kirishima.
Distribution: **JAPAN** (Shikoku; Kyushu).

Pedicia (Tricyphona) optabilis (Alexander, 1924)
1924 *T. optabilis* Alex., AESA, 17:70-1, type: Otaki, Chichibu, Saitama.
1954 *P. (T.) optabilis* Alex., PJS, 82:290, pl. 4, f. 32 (w).
Distribution: **JAPAN** (Hokkaido; Honshu; Shikoku; Kyushu).

Pedicia (Tricyphona) pectinata (Alexander, 1931)
1931 *T. pectinata* Alex., PJS, 44:354, pl. 1, f. 10 (w), type: Norikuradake, Japanese Alps, Shinano.
Distribution: **JAPAN** (Honshu; Shikoku).

Pedicia (Tricyphona) seticauda (Alexander, 1925)
1925 *T. seticauda* Alex., AM, (9)15:77-8, type:

Lake Ozenuma, on boundary between Iwashiro and Kotsuke.
Distribution: **JAPAN** (Hokkaido; Honshu; Shikoku; Kyushu).

Pedicia (Tricyphona) setipennis (Alexander, 1931)
1931 *T. setipennis* Alex., PJS, 44:355, pl. 1, f. 11 (w), type: Norikuradake, Japanese Alps, Shinano.
Distribution: **JAPAN** (Honshu).

Pedicia (Tricyphona) tenuiloba Alexander, 1957
1957 *P. (T.) tenuiloba* Alex., PJS, 85:354, 356-7, pl. 1, f. 2 (hyp), type: Kurokawa, Echigo.
Distribution: **JAPAN** (Honshu).

Pedicia (Tricyphona) vetusta (Alexander, 1913)
1913 *T. vetusta* Alex., Can. Ent., 45:318, 320-1, pl. 3, f. 5 (w), type: Tokyo.
Distribution: **JAPAN** (Hokkaido; Honshu; Shikoku).

Pedicia (Tricyphona) yakushimana (Alexander, 1930)
1930 *T. yakushimana* Alex., PJS, 42:67-8, pl. 1, f. 5 (w); pl. 2, f. 27 (hyp), type: Kosugidani, Yakushima.
1954 *P. (T.) yakushimana* Alex., PJS, 85:290.
Distribution: **JAPAN** (Shikoku; Kyushu).

Subgenus **NASITERNELLA** Wahlgren, 1904

1881 *Nasiterna* Wallengren, Ent. Tidskr., 2:179, type: *Limnobia variinervis* Zett., preocc. by *Nasiterna* Wagler, 1832.
1904 *Nasiternella* Wahlgren, Ark. Zool., 2, no. 7:4, type: *Limnobia variinervis* Zett.
1949 *Pedicia (Nasiternella)* Alex., Ark. Zool., 42A, no. 2:12.

Pedicia (Nasiternella) variinervis (Zetterstedt, 1851)
1851 *Limnobia variinervis* Zett., Dipt. Scandinaviae, 10:3813.
1869 *Amalopis variinervis* O. S., Mon. Dipt. N. Amer., 4:264.
1881 *Nasiterna variinervis* Wallengren, Ent. Tidskr., 2:191.
1934 *P. (N.) variinervis* Alex., PJS, 53:279.
Distribution: **EUROPE.**

subsp. **hokkaidensis** Alexander, 1934
1934 *P. (N.) hokkaidensis* Alex., PJS, 53:278-9, pl. 1, f. 7 (w); pl. 2, f. 29 (hyp), type: Sôunkyô.
1949 *P. (N.) variinervis hokkaidensis* Alex., Ark. Zool., 42A, no. 2:12.
Distribution: **JAPAN** (Hokkaido; Shikoku); **N. KOREA.**

Genus **NIPPONOMYIA** Alexander, 1924

1924 *Nipponomyia* Alex., IIM, 12:158-9, type: *Tricyphona kuwanai* Alex.
1935 *Nipponomyia* Alex., PJS, 56:551-2 (Key to spp.).

Nipponomyia kuwanai (Alexander, 1913)
1913 *Tricyphona kuwanai* Alex., Can. Ent., 45:318-9, pl. 3, f. 6 (w), type: Tokyo.
1920 *Tricyphona kuwanai* Alex., TAES, 46:14-5 (♂ description).
1924 *N. kuwanai* Alex., IIM, 12:159.
1935 *N. kuwanai* Alex., PJS, 56:552.
1950 *N. kuwanai* Esaki, Icon. Ins. Jap., ed. 2:1521, f. 4363.
Distribution: **JAPAN** (Honshu).

Nipponomyia trispinosa (Alexander, 1920)
1918 *Genus incertus* (Hexatomini), Brunetti, Rec. Ind. Mus., 15:328.
1920 *Tricyphona trispinosa* Alex., TAES, 46:15, type: possibly Kioto.
1924 *N. trispinosa* Alex., IIM, 12:159.
1935 *N. trispinosa* Alex., PJS, 56:552.
1950 *N. trispinosa* Esaki, Icon. Ins. Jap., ed. 2:1521, f. 4362.
Distribution: **JAPAN** (Honshu; Shikoku).

Genus **HETERANGAEUS** Alexander, 1925

1925 *Heterangaeus* Alex., AM, (9)15:78-9, type: *Polyangaeus gloriosus* Alex.

Heterangaeus esakii Alexander, 1925
1925 *H. esakii* Alex., AM, (9)15:79-80, type: Lake Ozenuma, on boundary between Iwashiro and Kotsuke.
Distribution: **JAPAN** (Honshu).

Heterangaeus gloriosus (Alexander, 1924)
1924 *Polyangaeus gloriosus* Alex., PJS, 24:569-71, type: Shimizu, Saghalien.
1925 *H. gloriosus* Alex., AM, (9) 15:79.
1938 *H. gloriosus*, var. Alex., PJS, 67:151.
Distribution: **SAGHALIEN; N. KOREA.**

subsp. **kusunokii** Alexander, 1954
1954 *H. gloriosus kusunokii* Alex., PJS, 82:290-1, pl. 4, f. 31 (w), type: Yuyama, near Matsuyama, Iyo.
Distribution: **JAPAN** (Shikoku).

Heterangaeus japonicus (ALEXANDER, 1919)
subsp. **japonicus** (ALEXANDER, 1919)
1919 *Polyangaeus japonicus* Alex., AESA, 18:342, type: Saitama.
1925 *H. japonicus* Alex., AM, (9) 15:79.
Distribution: **JAPAN** (Honshu; Shikoku; Kyushu).

subsp. **crenatus** ALEXANDER, 1933
1933 *H. japonicus crenatus* Alex., PJS, 51:541, type: Mt. Ohdai, Nara.
Distribution: **JAPAN** (Honshu).

Heterangaeus laticincta ALEXANDER, 1931
1931 *H. laticincta* Alex., PJS, 44:355-7, pl. 1, f. 12 (w), type: Hirayu, Japanese Alps, Shinano; Norikuradake, Japanese Alps, Shinano.
Distribution: **JAPAN** (Honshu).

Heterangaeus pallidellus ALEXANDER, 1933
1933 *H. pallidellus* Alex., PJS, 51:540-1, pl. 1, f. 21 (w), type: Mt. Kurobegoro, Echiu.
Distribution: **JAPAN** (Honshu).

Heterangaeus spectabilis ALEXANDER, 1925
1925 *H. spectabilis* Alex., AM, (9) 15:80-1, type: Hinoëmata, Iwashiro.
Distribution: **JAPAN** (Honshu).

Genus **DICRANOTA** ZETTERSTEDT, 1838
1838 *Dicranota* Zett., Ins. Lapponica, Dipt., 851, type: *Dicranota guerini* Zett.
1949 *Dicranota* Alex., Ark. Zool., 42A, no. 2:17-8 (Key to subgenera).

Key to Subgenera

1. Wings with supernumerary crossveins in certain of the cell ·····2
   No supernumerary crossveins in any cells of wing ·····**Rhaphidolabis**
2. A supernumerary crossvein in cell R_1, no other crossveins present ·····3
   No supernumerary crossvein in cell R_1; at least one such vein in cell R_2···**Dicranotella**
3. Cell *1st* M_2 closed ····· **Eudicranota**
   Cell *1st* M_2 open ····· **Dicranota,** s. str.

Subgenus **DICRANOTA,** s. str.

Dicranota (Dicranota) nippoalpina ALEXANDER, 1933
1933 *D.* (*D.*) *nippoalpina* Alex., PJS, 50:147-8, pl. 1, f. 14 (w); pl. 3, f. 42 (hyp), type: Shiroumadake, Japanese Alps.
Distribution: **JAPAN** (Honshu).

Dicranota (Dicranota) nipponica ALEXANDER, 1919
1919 *D. nipponica* Alex., AESA, 12:344, type: Meguro, Tokio.
Distribution: **JAPAN** (Honshu).

Dicranota (Dicranota) sicaria ALEXANDER, 1947
1947 *D.* (*D.*) *sicaria* Alex., AESA, 40:354, type: Hamasaka, Hyogo.
Distribution: **JAPAN** (Honshu).

Dicranota (Dicranota) yezoensis ALEXANDER, 1924
subsp. **yezoensis** ALEXANDER, 1924
1924 *D. yezoensis* Alex., PJS, 24:571, type: Lake of Akan.
Distribution: **JAPAN** (Hokkaido).

Subgenus **DICRANOTELLA** ALEXANDER, 1949
1949 *Dicranota* (*Dicranotella*) Alex., Ark. Zool., 42A, no. 2:18, type: *Rhaphidolabina sibirica* Alex. (not *siberica*).

Dicranota (Dicranotella) nebulipennis ALEXANDER, 1936
1936 *D.* (*Amalopina*) *nebulipennis* Alex., PJS, 60:183-4, pl. 1, f. 10 (w); pl. 2, f. 30 (hyp), type: Iwate-gun, Iwate.
1949 *D.* (*D.*) *nebulipennis* Alex., Ark. Zool., 42A no. 2:18.
Distribution: **JAPAN** (Honshu).

Subgenus **EUDICRANOTA** ALEXANDER, 1934
1934 *Dicranota* (*Eudicranota*) Alex., in Curran, Keys to the Families and Genera of North American Diptera, p. 40, type: *Dicranota notabilis* Alex.
1949 *Dicranota* (*Eudicranota*) Alex., Ark. Zool., 42A, no. 2:17-8.

Dicranota (Eudicranota) dicranotoides (ALEXANDER, 1924)
1924 *Rhaphidolabina dicranotoides* Alex., AESA, 17:72-3, type: Mt. Takao, Musashi.
1935 *D.* (*Amalopina*) *dicranotoides* Alex., PJS, 56:358 (Key to Japanese spp. of *Amalopina*).
1949 *D.* (*E.*) *dicranotoides* Alex., Ark. Zool., 42A, no. 2:18.
Distribution: **JAPAN** (Honshu; Shikoku).

Subgenus **RHAPHIDOLABIS** OSTEN SACKEN, 1869
1869 *Rhaphidolabis* O. S., Mon. Dipt. N. Amer., 4:284-7, type: *Rhaphidolabis tenuipes* O. S.
1949 *Dicranota* (*Rhaphidolabis*) Alex., Ark. Zool., 42A, no. 2:18.

Dicranota (Rhaphidolabis) angulata ALEXANDER, 1936

1936 *D.* (*R.*) *angulata* Alex., PJS, 60:182-3, pl. 1, f. 9 (w), type: Iwate-gun, Iwate.
Distribution: **JAPAN** (Honshu).

Dicranota (**Rhaphidolabis**) **clausa** ALEXANDER, 1938
1938 *D.* (*R.*) *clausa* Alex., PJS, 66:115-7, pl. 1, f. 13 (w); pl. 3, f. 38 (hyp), type: Matsuo, Iwate.
1953 *D.* (*R.*) *clausa* Alex., PJS, 82:61-2, pl. 2, f. 17 (w).
Distribution: **JAPAN** (Honshu; Shikoku).

Dicranota (**Rhaphidolabis**) **consors** (ALEXANDER, 1923)
1923 *R. consors* Alex., AESA, 16:68-9, type: Tamagawa, Saitama.
1954 *D.* (*R.*) *consors* Alex., PJS, 82:291, pl. 4, f. 37 (hyp).
Distribution: **JAPAN** (Honshu; Shikoku; Kyushu).

Dicranota (**Rhaphidolabis**) **flavibasis** (ALEXANDER, 1919)
subsp. **flavibasis** (ALEXANDER, 1919)
1919 *R. flavibasis* Alex., AESA, 12:343, type: Meguro, Tokio.
Distribution: **JAPAN** (Honshu); **SAGHALIEN.**

Dicranota (**Rhaphidolabis**) **gibbera** (ALEXANDER, 1921)
subsp. **gibbera** (ALEXANDER, 1921)
1921 *Rhaphidolabina gibbera* Alex., AESA, 14:121, type: Gifu.
1924 *Rhaphidolabina gibbera* Alex., PJS, 24:569.
1930 *D.* (*Amalopina*) *gibbera* Alex., PJS, 42:520, pl. 1, f. 12 (w).
1930 *D.* (*Amalopina*) *gibbera*, var. Alex., PJS, 43:508.
1935 *D.* (*Amalopina*) *gibbera gibbera* Alex., PJS, 56:358 (Key to Japanese spp. of *Amalopina*).
1938 *D.* (*Amalopina*) *gibbera gibbera* Alex., PJS, 66:322 (Key to spp. of *elegantula* group).
1949 *D.* (*R.*) *gibbera* Alex., Ark. Zool., 42A, no. 2:18.
1950 *Amalopina gibbera* Esaki, Icon. Ins. Jap., ed. 2:1521, f. 4364.
Distribution: **JAPAN** (Hokkaido; Honshu; Shikoku; Kyushu); **SAGHALIEN**; **FORMOSA.**

Dicranota (**Rhaphidolabis**) **idiopyga** ALEXANDER, 1953
1953 *D.* (*R.*) *idiopyga* Alex., PJS, 82:62-3, pl. 2, f. 12 (hyp), type: Mt. Tsurugi, Kawati to Minokosi & Minokosi to Nagoro, Awa.
Distribution: **JAPAN** (Shikoku).

Dicranota (**Rhaphidolabis**) **macracantha** ALEXANDER, 1947
1947 *D.* (*R.*) *macracantha* Alex., AESA, 40:354-5, type: Kamikochi, Shinano.
Distribution: **JAPAN** (Honshu).

Dicranota (**Rhaphidolabis**) **ontakensis** ALEXANDER, 1947
1947 *D.* (*R.*) *ontakensis* Alex., AESA, 40:355-6, type: Ontake, Hida.
Distribution: **JAPAN** (Honshu).

Dicranota (**Rhaphidolabis**) **paraconsors** ALEXANDER, 1955
1955 *D.* (*R.*) *paraconsors* Alex., AESA, 48:372, type: Yatsugatake, Shinano.
1957 *D.* (*R.*) *paraconsors* Alex., PJS, 85:357, pl. 1, f. 1 (w); f. 6 (hyp).
Distribution: **JAPAN** (Honshu).

Dicranota (**Rhaphidolabis**) **persessilis** ALEXANDER, 1954
1954 *D.* (*R.*) *persessilis* Alex., PJS, 82:292-3, pl. 4, f. 33 (w), type: Mt. Saragamine, Iyo.
Distribution: **JAPAN** (Shikoku).

Dicranota (**Rhaphidolabis**) **platymera** ALEXANDER, 1934
1934 *D.* (*R.*) *platymera* Alex., PJS, 53:279-80, pl. 1, f. 8 (w); pl. 2, f. 30 (hyp), type: Yumoto, Shimotsuke.
Distribution: **JAPAN** (Honshu).

Dicranota (**Rhaphidolabis**) **polymera** ALEXANDER, 1933
1933 *D.* (*R.*) *polymera* Alex., PJS, 51:537-8, pl. 1, f. 18 (w); pl. 3, f. 39 (hyp), type: Wakasugiyama, Chikuzen.
1954 *D.* (*R.*) *polymera* Alex., PJS, 82:292 (♀ description).
Distribution: **JAPAN** (Shikoku; Kyushu).

Dicranota (**Rhaphidolabis**) **profunda** ALEXANDER, 1950*
1950 *D.* (*Dicranota*) *profunda* Alex., AESA, 42:425-6, type: Funakoshi, Iwate.
Distribution: **JAPAN** (Honshu).

Dicranota (**Rhaphidolabis**) **spina** ALEXANDER, 1933
1933 *D.* (*R.*) *spina* Alex., PJS, 51:398-9, pl. 1, f. 17 (w); pl. 4, f. 48 (hyp), type: Mt. Kurobegoro, Echiu.
Distribution: **JAPAN** (Hokkaido; Honshu).

---

*Reference to *Rhaphidolabis* is according to Prof. Dr. ALEXANDER, who kindly adviced for my unpublished check list of Japanese Tipulidae.

Dicranota (Rhaphidolabis) subconsors (ALEXANDER, 1924)
1924 *R. subconsors* Alex., PJS, 24:571-2, type: Lake Shikotsu.
Distribution: **JAPAN** (Hokkaido).

Dicranota (Rhaphidolabis) tuberculata ALEXANDER, 1936
1936 *D. (R.) tuberculata* Alex., PJS, 59:241-2, pl. 1, f. 13 (w), type: Kibune, Kyoto.
Distribution: **JAPAN** (Honshu).

Genus **ULA** HALIDAY, 1833

1833 *Ula* Haliday, Ent. Mag., 1:153, type: *Limnobia macroptera* Macq. (as *mollissima*, sp. nov.).
1864 *Macroptera* Lioy, Atti Inst. Veneto, (3) 9:224, type: *Limnobia macroptera* Macq.
1954 *Ula* Tokunaga, Ishida et Nobuchi, Sci. Rep. Saikyo Univ., Agric., 6:1-10, 19 figs. (Key to Japanese spp.).

Subgenus **ULA**, s. str.

Ula (Ula) cincta ALEXANDER, 1924
1924 *U. cincta* Alex., PJS, 24:573, type: Akan; Teppetsu.
1954 *U. cincta* Nobuchi, Sci. Rep. Saikyo Univ., Agric., 6:2, 3, 4-5, f. 1 (♂w); f. 5(hyp); f. 8-13 (larva); f. 18-19 (pupa).
Distribution: **JAPAN** (Hokkaido; Honshu; Shikoku).

Ula (Ula) fungicola NOBUCHI, 1954
1954 *U. fungicola* Nobuchi, Sci. Rep. Saikyo Univ., Agric., 6:2, 3, 5-6, f. 2 (♂ w); f. 6 (hyp), type: Takayama, Gifu.
Distribution: **JAPAN** (Honshu).

Ula (Ula) kiushiuensis ALEXANDER, 1933
1933 *U. kiushiuensis* Alex., PJS, 51:541-2, pl. 1, f. 22 (w); pl. 3, f. 40 (hyp), type: Sobosan, Bungo.
1954 *U. kiushiuensis* Nobuchi, Sci. Rep. Saikyo Univ., Agric., 6:3.
Distribution: **JAPAN** (Kyushu).

Ula (Ula) longicellata ISHIDA, 1954
1954 *U. longicellata* Ishida, Sci. Rep. Saikyo Univ., Agric., 6:3-4, 7-8, f. 4 (♀w), type: Kurami, north of Mimasaka-Kamo, Tomada-gun, Okayama.
Distribution: **JAPAN** (Honshu).

Ula (Ula) perelegans ALEXANDER, 1924
1924 *U. perelegans* Alex., PJS, 24:572-3, type: Abashiri.
1954 *U. perelegans* Nobuchi, Sci. Rep. Saikyo Univ., Agric., 6:2, 3, 4.
Distribution: **JAPAN** (Hokkaido).

Ula (Ula) shiitakea NOBUCHI, 1954
1954 *U. shiitakea* Nobuchi, Sci. Rep. Saikyo Univ., Agric., 6:3, 4, 6-7, f. 3 (♂ w); f. 7 (hyp); f. 14-17 (larva), type: Kibune, Kyoto.
Distribution: **JAPAN** (Honshu).

Ula (Ula) succincta ALEXANDER, 1933
1933 *U. succincta* Alex., PJS, 51:400, pl. 1, f. 19 (w); pl. 4, f. 49 (hyp), type: Mt. Mitake, Musashi.
1954 *U. succincta* Nobuchi, Sci. Rep. Saikyo Univ., Agric., 6:3, 4.
Distribution: **JAPAN** (Honshu).

(*To be continued*)

(Entomological Laboratory of Kakogawa Branch, Received Aug. 23, 1958)

昭和33年12月20日 印刷
昭和33年12月25日 発行

兵庫農科大学研究報告 第3巻 第2号
自然科学編

編集兼発行 兵庫農科大学
兵庫県多紀郡篠山町

印刷所 神戸市長田区西尻池町5丁目13
(株) 高田印刷紙器工廠
高田一市
電話神戸⑦(代表)2623